FOSSIL ENERGY

DOE/BC/15107-1
(OSTI ID: 773160)

ENHANCING THE EFFECTIVENESS OF CARBON DIOXIDE FLOODING BY MANAGING ASPHALTENE PRECIPITATION

Annual Report
September 10, 1999-September 30, 2000

By
Milind Deo

Date Published: January 2001

Work Performed Under Contract No. DE-AC26-98BC15107

University of Utah
Salt Lake City, Utah

National Petroleum Technology Office
U.S. DEPARTMENT OF ENERGY
Tulsa, Oklahoma

DOE/BC/15107-1
Distribution Category UC-122

Enhancing the Effectiveness of Carbon Dioxide Flooding by Managing Asphaltene Precipitation

By
Milind Deo

January 2001

DE-AC26-98BC15107

Prepared for
U.S. Department of Energy
Assistant Secretary for Fossil Energy

Dan Ferguson, Project Manager
National Petroleum Technology Office
P.O. Box 3628
Tulsa, OK 74101

Prepared by
Department of Chemical and Fuels Engineering
University of Utah
1471 Federal Way
Salt Lake City, UT 84112

Table of Contents

List of Figures

List of Figures

Abstract

The objectives of this project were identify conditions at which carbon dioxide induced precipitation occurred in crude oils. Establishing compositions of the relevant liquid and solid phases was planned. Other goals of the project were to determine if precipitation occurred in cores and to implement thermodynamic and compositional models to examine the phenomenon. Exploring kinetics of precipitation was also one of the project goals. Crude oil from the Rangely field (eastern Colorado) was used as a prototype. All of the planned activities were completed.

Rangely crude oil contains only about 1 wt% asphaltenes initially. It was determined using single-contact experiments that CO_2-induced precipitation is also of the same order as the initial amount of asphaltenes in the crude, for these light oils. Experiments showed that the onset of precipitation was between 20-30 mole% CO_2. Amount of precipitation increased moderately with increased CO_2 concentration. As gas added to the mixture, for the same CO_2 concentrations, about 1.5 to 2 times the dead-oil precipitation amount was obtained. It was also shown that multiple contacts with CO_2 which are a natural consequence of the CO_2 miscible flooding process increase the amount of precipitate as well by 1.5 to 2 times (compared to the dead-oil single contact precipitation). Analyses of the precipitate revealed that the molecular weights of the compounds in the precipitate ranged from about 250-900 with an average of about 750. The particle sizes depended on the process and path of precipitation and were in the 10-20 micron range.

Coreflooding experiments completed earlier showed that multiple contact miscibility was achieved, as expected. The multiple contact mixture, having been enriched in intermediates forms 1.5 to 2 times as much precipitate in comparison to equivalent single-contact mixtures. There was no loss of permeability. Thin sections of the core examined after the flood revealed that there was essentially no deposition in the core. This could be related to the small sizes of the asphaltene molecules in comparison to the average pore sizes.

In order to consider the fact that smaller molecular weight compounds are also part of the solids, a new thermodynamic model was developed. This was accomplished by combining the principles of asphaltene and wax precipitation models. Results using the new model matched experimental results better than the previous models.

Kinetic measurements were performed and first-order kinetic constants were derived. Models for precipitation and agglomeration were reviewed.

Preliminary compositional simulations showed the effect of pressure on oil recovery.

Executive Summary

The report is organized into six sections:

- Single and multiple contact experiments with the Rangely crude oil
  In this section, all the thermodynamic experiments are described. Basic literature in the area is reviewed.
- Thermodynamic modeling
  In this section, more common asphaltene precipitation models have been reviewed and a new model has been developed.
- Pure component experiments and modeling
  In this section, pure component experiments and simple models to match experimental data are described. These experiments were performed to establish parallels between solubility behavior of polyaromatic compounds in hydrocarbon solvents and asphaltenes in crude oils.
- Kinetic experiments and modeling
  A variety of kinetic experiments are described here along with appropriate models.
- Corefloods
  A special coreflood was conducted to simulate the wellbore conditions, where the multiple contact mixture was "flashed" at wellbore pressure – keeping the temperature constant. This experiment and results are described in this section.
- Compositional simulations
  Results of preliminary compositional simulations are described.

Pertinent conclusions are drawn in each of the sections. A reference list is included at the end of the report.

Single and Multiple Contact Experiments With the Rangely Crude Oil

Synopsis

Precipitation of solids, believed to be asphaltenes is common in most carbon dioxide floods. The oils in most carbon dioxide flood applications, however, are light crudes with low initial asphaltene content. Precipitation is common after carbon dioxide breakthrough in production equipment. It is believed that precipitation does not occur in the reservoir. The objective of this paper was to identify the reasons for this phenomenon. The mature carbon dioxide flood at Rangely field in Colorado was selected as an example.

A high-pressure, high-temperature pressure-volume-temperature apparatus in conjunction with a high-pressure core flooding system was used to study carbon dioxide induced precipitation from the Rangely crude oil. Rangely crude contains about 1% heptane insolubles. It was determined that first-contact precipitation, at different carbon dioxide concentrations was negligible. Core flooding experiments at field conditions revealed that precipitation did occur at the core exit. This essentially showed that the precipitation phenomenon in crudes that are likely CO_2-flood candidates is due to the multiple contact process and the associated compositional changes. Multiple contact experiments conducted to prove this hypothesis showed that multiple contact precipitation amounts were 3-5 times the first-contact precipitation values. The compositional changes (in the original crude) to cause widespread precipitation were established.

The precipitates from the field and various laboratory experiments were analyzed using GC and SARA, which showed that field precipitates contained compounds other than original heptane insolubles and also exhibited some unique features.

Introduction

Asphaltenes by definition are a compound class. Even though precipitation has been observed in most CO_2 flooding applications, there is uncertainty with respect to the thermodynamic conditions that lead to precipitation. The differences between asphaltenes or solids precipitated by different means are also not well established.

Asphaltene content in the crude as determined by conventional methods is not a good indicator of asphaltene precipitation problems. It has been reported that a crude with more than 17 wt % asphaltenes did not have asphaltene problems, while a crude with only 0.1 wt % had serious asphaltene deposition problems (Kokal and Sayegh, 1995). Asphaltenes precipitate because of changes of pressure, temperature and composition and the thermodynamic instability that these changes entail.

The use of carbon dioxide to increase oil recovery has received considerable attention. In United States, there were 60 active miscible CO_2 projects in operation in 1996, whereas in Canada there were 40 hydrocarbon miscible active projects (Srivastava and Huang, 1997). It has been projected that CO_2 miscible flooding potentially could recover as much as 40% of the total oil to be recovered by all enhanced recovery methods (Stalkup, 1978).

Carbon Dioxide is highly soluble in oil and to a lesser extent in water. Carbon dioxide improves oil recovery by the following mechanisms: reduction in crude oil viscosity and increase in water viscosity; swelling of crude oil; reduction in oil density; and miscibility effects. The miscibility between the oil and CO_2 or hydrocarbon solvents eliminates interfacial tension and capillary forces and could help recover, in theory, all of the residual oil.

When the injection gas and reservoir oil, mixed in any ratio, form a single phase, they are said to be first contact miscible. First contact miscibility can be achieved only for highly hydrocarbon rich gases, or at very high pressures for lean systems. Carbon dioxide is not first contact miscible with most reservoir oils even at fairly high operating pressures. CO_2 can develop miscibility through multiple contacts under specific conditions of pressure and temperature and specific oil compositions. One of the mechanisms for generating miscibility is the vaporizing gas drive process (VGD) in which the gas phase is getting enriched through extraction of the light and intermediate fractions of oil. The original oil is in contact with the vapor phase generated from the previous mixture. The vapor phase eventually gets so rich in light and intermediate hydrocarbons that it becomes completely miscible with the reservoir crude. Minimum pressure required to achieve this is called the minimum miscibility pressure (MMP). Carbon dioxide flooding is typically a VGD process, which is shown schematically in Figure 1.

Previous Experimental Studies

Gas injection processes are simulated in batch type tests. These tests generate the volumetric and compositional data required for evaluation and calibration of phase behavior models. The most common experiment is the swelling test, or single contact gas injection. A known amount of oil is loaded into an equilibrium cell and the injection gas is progressively added to the oil by steps. Saturation pressures, phase compositions and phase volumes are measured as necessary. These type of tests are also used in measuring high-pressure carbon dioxide induced solids precipitation.

Burke et al. (1990) obtained experimental asphaltene precipitation data from static precipitation tests in which several oil and solvent mixtures were evaluated in a high pressure cell at reservoir temperature and pressure. Burke et al. (1990) showed that precipitation would depend on the composition of the crude oil, the added solvent, and the concentration of asphaltenes in the oil. Results show that temperature, pressure, and the phase behavior of the system also influence asphaltene precipitation. In static PVT tests, asphaltene flocculation usually occurs, whereas in corefloods, asphaltene precipitation/deposition in the core matrix may not occur. It was reported (Nighswander, et al., 1993) that it has been observed that a number of reservoir oils that exhibit severe asphaltene formation when mixed with miscible injection solvents in static test cells do not suffer from adverse effects during dynamic displacement experiments. However, it has also been observed that some oils that do not exhibit severe asphaltene formation in static cells do exhibit altered behavior in dynamic experiments.

Graue and Zana (1981) reported asphaltene precipitation in the extensive laboratory evaluation undertaken to evaluate the performance of a possible CO_2 tertiary project at Rangely Weber Sand Unit in Colorado. Precipitation occurred at gas concentration of 44 mole % or higher with an injection gas (95 mole % CO_2 and 5 mole % CH_4), while with a second gas (85 mole % CO_2, 5 mole % CH_4, and 10 mole % N_2), it occurred at gas concentration as low as 25 mole % (lowest gas concentration studied). The solid precipitation was estimated to be 2 to 5 vol % of the original reservoir oil. Hervey and Iakovakis (1991) reported that deposits have been found in pumps, tubing, wellheads, flowlines, and workover equipment, with no evidence of asphaltene precipitation in the formation (in Rangely).

Hirschberg et al. (1984) studied the influence of temperature and pressure on asphaltene precipitation during natural depletion. They found that when CO_2 was injected into the crude oil no precipitation was observed without addition of decane, an intermediate hydrocarbon component. They also concluded that precipitation is highest at bubble point pressure.

Monger and coworkers (1987, 1991) provided the most comprehensive database on precipitation associated with CO_2 recovery. They observed precipitation for mixtures containing between 70 and 96 mole% of CO_2. It was observed that the development of miscibility is associated with the formation of the solid phase. Novosad and Constain (1990) observed precipitation at 40 - 50 mole % CO_2 concentrations. Srivastava et al. (1995) indicated that asphaltenes began to flocculate at about 42 mole % CO_2 concentration, and after that, there was a linear increase in asphaltene flocculation with CO_2 concentration. Thus, there is no consensus on the CO_2 concentrations required to induce precipitation. The relationship between precipitation during first and multiple contact has also not been studied.

Precipitating tendencies of first contact mixtures are likely to be significantly different from the multiple contact mixtures, which are much richer in hydrocarbon intermediates. Understanding this difference is one of the aims of this study.

Experimental System and Procedure

Experiments in this study were carried out in a high-pressure high-temperature equipment illustrated in Figure 2. The system was designed for temperatures up to 300 °F and pressures up to 5,000 psi permitting the experiments to be run at reservoir conditions. One important characteristic of this system is that it does not use mercury as the isobaric displacement fluid.

The equipment consists of four major components: heating system, fluid displacement, visual pressure-volume-temperature (PVT) cells and the sampling system. The set temperature ($\pm 2^{\circ}F$) for an experiment is obtained by placing the equipment in an insulated wooden box. This box uses a heater, circulating fan, thermocouple, and a thermostat to regulate temperature. A coaxial heating cable is used to regulate the temperature of the circulating pump that is placed outside.

The fluid displacement section is used to supply the fluids: oil, CO_2 and water to the PVT cells. This section is composed of three moveable piston vessels (volume: one liter

each) to store the fluids, a low pressure input to feed the required fluids to the vessels and two hydraulic pumps connected to the vessels to transfer fluids from each of these vessels. The hydraulic pumps used are high-pressure precision positive displacement pumps. These pumps allow careful control of pressure, flow rate, and volume during displacement. The outlets of the vessels are connected to the manifolds which permit filling and discharging all fluids to different parts of the system in a flexible manner. The PVT cells have transparent windows on either side, which are useful in visualizing the ongoing experiment. These cells are connected to a circulating pump allowing equilibration of the system fluids.

The outlet from the PVT cells is connected to three sets of parallel high pressure in-line filters; each line has filters in series with pore sizes of 2 and 0.5 microns respectively to trap solids for quantitative analysis of the solid phase. There is also a bypass line to the filters. The system pressure is maintained with a special back-pressure regulator (BPR). The BPR was specially built to work with liquid and superfluid CO_2. The high-pressure sample exiting the BPR is received into a series of sampling cylinders. The liquid and the gas are separated for quantitative and compositional analyses.

Four different types of thermodynamic experiments were conducted.

- First contact experiments with dead oil.
- First contact experiments with live oil.
- Simulated multiple contact experiments (by adding an intermediate light cut to the live oil).
- True multiple contact experiments.

All the experiments were conducted at a constant temperature of 160 °F. Once the desired equilibrium conditions are established in the PVT cells, isobaric displacements to the sampling systems are undertaken through the filter lines using carbonated brine. The filters are repeatedly washed with supercritical CO_2 to remove occluded oil. The volumes of oil, gas and CO_2 needed to perform all the experiments are calculated using appropriate component properties. Thermodynamic calculations are used to guide the mixing process.

True multiple contact miscibility is achieved by vaporizing gas drive mechanism (forward contacts) in which the gas phase is getting enriched through extraction of the light and intermediate fractions of oil (Figure 1). The overall composition of the oil-CO_2

mixture for the first contact was 76 mole% CO_2 and 24 mole% dead oil. This mixture is equilibrated in one of the PVT cells at a pressure below the bubble point of this mixture. Most of the vapor phase from this mixture is transferred isobarically to the second PVT cell which already contains fresh crude essential for the second contact. The remaining mixture in the first PVT cell is displaced through the high pressure filters into the fluid sampling system. The vapor phase from the second contact is displaced in a similar fashion into a third-contact PVT cell (the first PVT cell was prepared to be the third contact cell, once all the sample was displaced from it). Prior to this displacement, this PVT cell also was charged with the necessary crude oil. Remainder of the sample from the second contact was displaced through a separate line of filters into the fluid sampling system. Third contact yielded miscibility. Solid, liquid and gas sampling procedures were repeated for the third contact.

Results and Discussion

Original crude oil

The carbon number distribution for the oil from the Rangely field is shown in Figure 3. The C_5-C_{60} distribution is shown in the figure. The oil contained 3.75 wt% C_{60}+. The gravity of the oil was about 34° API. Thus, Rangely oil is basically a light crude oil. The SARA (saturates, aromatics, resins and asphaltenes) fractionation of the crude is shown in Figure 4. The procedure to obtain SARA fractions was modified (slightly different solvent amounts) from the well-established methods (Speight, 1999). The asphaltene fraction of the oil as determined as n-pentane insolubles was found to be 2.83 wt%. n-heptane insoluble fraction, determined independently was 1.51 wt%.

First contact experiments – Dead oil.

In first-contact experiments with carbon dioxide, the crude oil and CO_2 mixtures in different molar proportions were charged to the PVT cell. The bubble points of the mixtures were measured and the mixtures were displaced through online, high-pressure filters at a constant pressure above their respective bubble points. The temperature in all the experiments was maintained at 160°F.

The amounts of precipitates at various CO_2 concentrations are shown in Figure 5. The solids were collected from the filters and also from the PVT cells. About 70% of the solids were from the filters. Based on these results, the precipitation onset was determined to be between 20-30%, which is consistent with the findings reported by Graue and Zana (1981). The amounts are less than 1% even at CO_2 concentrations of 76 mole%. It can be observed that the precipitation amounts are comparable to heptane insolubles in the oil.

The solids compositions, as determined from the SARA analysis (for the experiment with 50 mole% CO_2) are shown in Figure 6. Solids from the filters and those collected the PVT cell (as residual depositions after the experiment) differed slightly in composition. Pentane insolubles were about 40% showing that other fractions also constitute a significant portion of solids.

First contact experiments – Live oil

In the live oil experiments, the gas to oil ratio (GOR) was kept constant at 155 scf/stb. The gas composition is shown in Table 1. Amounts of precipitates at varying CO2 concentrations are shown in Figure 7. For the same CO2 concentration (with respect to the dead oil), the precipitated amount is 3 to 4 times that of the precipitate from the dead oil experiments. Compositions of the precipitate were similar to the solids compositions (SARA) from the dead oil. The asphaltenes (pentane insolubles) in the oil after the precipitation experiment are shown in Figure 8. At lower CO_2 concentrations, the asphaltene amounts are comparable to those from the original crude oil; however, at higher CO_2 concentrations lower amount of asphaltenes are obtained. The crude oil at the time of the test, has lost some of the heavier components and also some of the lighter components to the flashed gas phase. The relative importance of these two competing effects determines the asphaltene content of the oil from which CO_2 induced precipitation has already occurred.

Simulated multiple contact experiments

In the carbon dioxide multiple contact process, the oil just before attainment of miscibility is enriched with intermediates (Orr et al., 1981). In order to simulate this effect without undertaking true multiple contact tests, a light cut from the crude oil itself

was added to the oil. For this experiment, an ASTM D-2886 distillation column was first used to generate a C_{15}- fraction from the Rangely crude. The Rangely oil was distilled to an upper boiling point of 520°F. The cumulative carbon number distribution for this distillation cut is shown in Figure 9. It can be observed from Figure 9 that about 84% of the cut is below C_{15}. The fraction added to the oil to simulate multiple-contact composition amounted to 30% (molar) with respect to the live oil and 48% with respect to the dead oil. The precipitation with the addition of the light-intermediate fraction to the oil is also plotted in Figure 10. With the addition of the "light – intermediate" fraction, amount of precipitate is approximately twice the amount for equivalent CO_2 concentration without the cut (compared to the live oil precipitates). This suggests that multiple-contact mixtures are likely to yield twice the amount of precipitate expected through first-contact experiments. With the addition of the light-cut, the precipitation is also more sensitive to CO_2 concentrations and increases more rapidly as CO_2 concentration goes up.

The precipitates contain about 5% more asphaltenes than the precipitates from the dead or live oils, indicating that the solids are slightly more polar and of higher molecular weight.

True multiple contact experiments

The procedure for true forward multiple contact experiments is described in the previous section. In the first PVT cell (first contact), 76 mole% CO_2 was mixed with 24% oil. A two-phase mixture resulted from this contact at 1475 psia and 160°F. Upper phase occupied 70% by volume of the cell (total volume of 77 cc). From this cell, 90 vol% of the upper phase was mixed with fresh crude in the second contact to produce a total of 77 cc. 45% of the cell after this contact contained the gas phase. 90% by volume of this cell was displaced into the third contact cell, once again to produce a total of 77 cc. Complete miscibility was obtained in the third contact cell at 1400 psia. The molar concentrations of CO_2 and crude oil in the first and in subsequent contacts are shown in Table 2. In a constant volume PVT cell, the overall CO_2 concentration in subsequent contacts decreases. The amounts of precipitates with multiple contacts are compared to the first contact amounts in Figure 11. The multiple contact amounts are about two to three times the first contact amounts for the same CO_2 concentration.

Analyses of the Precipitates using TOF-SIMS and GC-MS

Solid samples from previous thermodynamic experiments were analyzed using the Time of flight Mass Spectrometer (TOF-SIMS). Preliminary analyses indicate that signatures of asphaltenes precipitated from different oils, and at different conditions had similar "signatures". Second significant finding was that the concentrations of higher molecular weight compounds (> 800 molecular weight) were extremely small.

TOF-SIMS was used on asphaltene samples from the Rangely oil field and from the asphaltenes precipitated from oil from Phillips Petroleum Company (a more asphaltic crude oil from southern Utah). The positive ion images from the two samples are shown in Figures 12 and 13. The intensities have been plotted at three different mass ranges in the two figures. The two signatures are very similar. Even though the relative intensities at different masses vary for the two samples, the peaks occur at identical locations. Considering that the oils are from two completely different fields and that the solids analyzed were precipitated by completely different means (one was a field sample and the other generated in our laboratories using single-contact CO_2 experiment), this finding is extraordinary.

Conclusions

About 20-25% CO_2 molar concentration is necessary to induce measurable precipitation in crude oils containing originally low quantities of asphaltenes. Live oils yielded significantly higher amounts of precipitates than equivalent dead oils. A hypothesis that multiple contact mixtures yielded significantly higher amounts of precipitates was conclusively proven based on results from simulated multiple contact (addition of an intermediate cut) and true multiple contact experiments.

Table 1: Gas composition in the live oil experiment

Component	Mole%
Methane	91.1
Ethane	3.7
Propane	5.2

Table 2: Parameters of the true multiple contact experiment (mole%)

Contact	CO_2	Oil
First	76	24
Second	67	33
Third	54	46

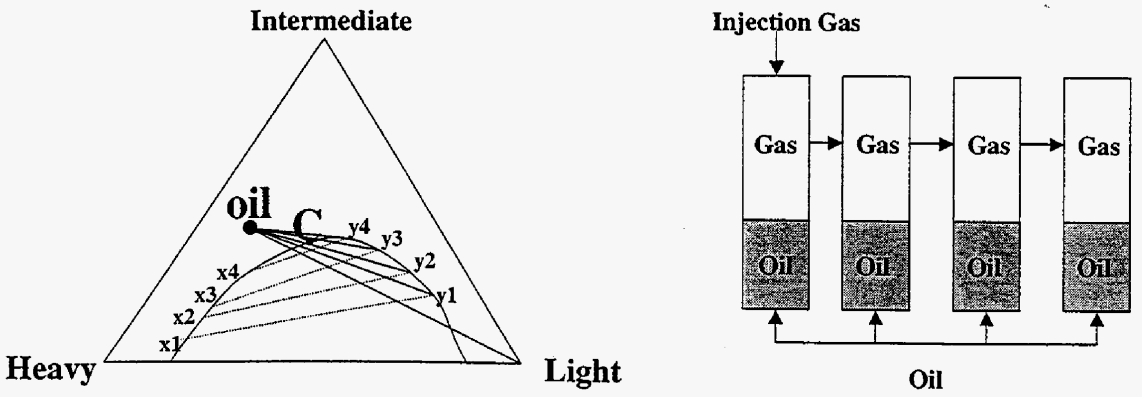

Figure 1:Diagram showing the development of forward multiple contact miscibility on a ternary plot and in an experimental cell

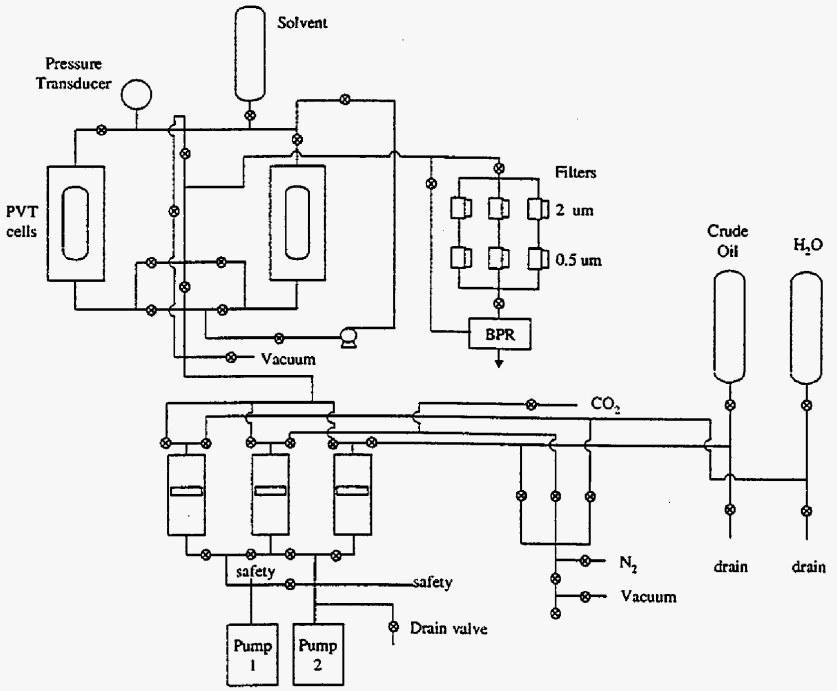

Figure 2: Experimental system used to study solids precipitation with first and multiple contact experiments

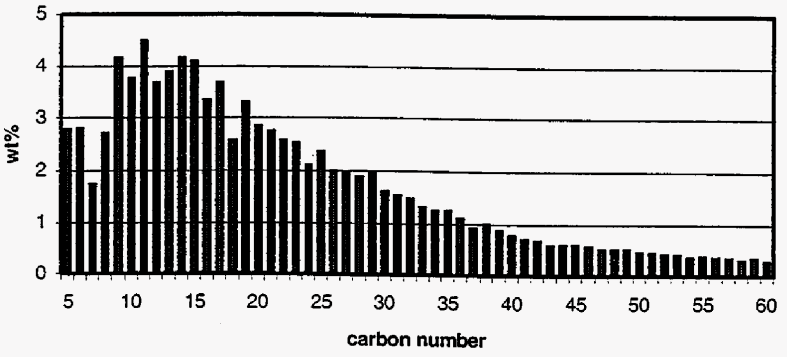

Figure 3: Carbon number distribution of the original crude oil

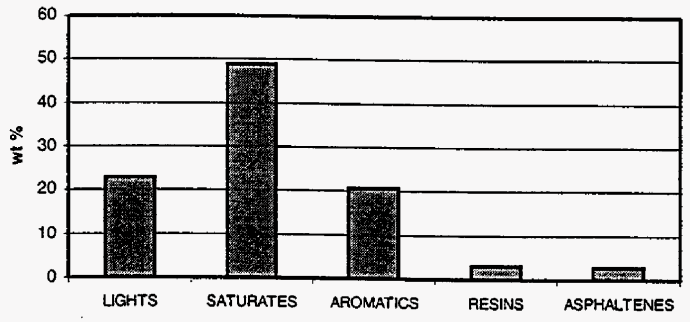

Figure 4: Saturates-aromatics-resins and asphaltenes distributions in the original crude oil

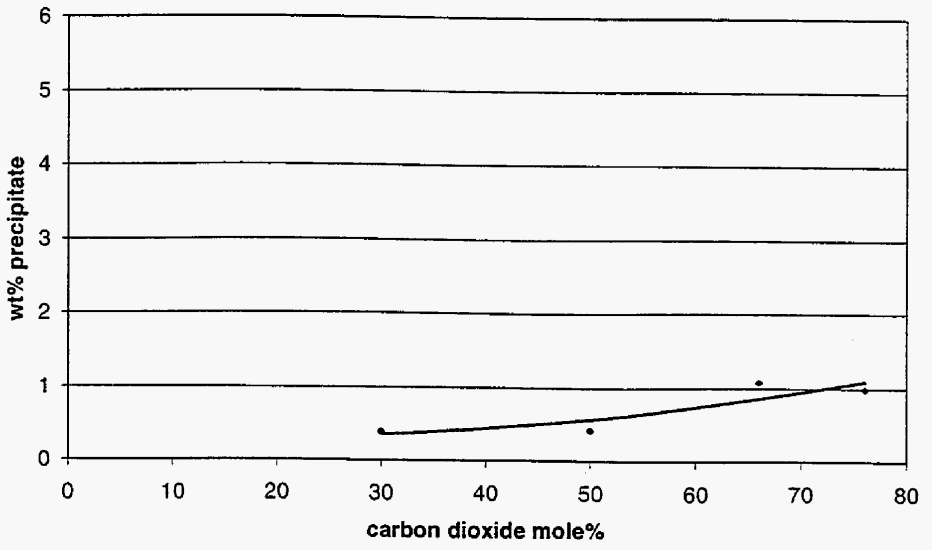

Figure 5: Precipitation amounts with varying carbon dioxide concentrations; first-contact experiments with dead oil

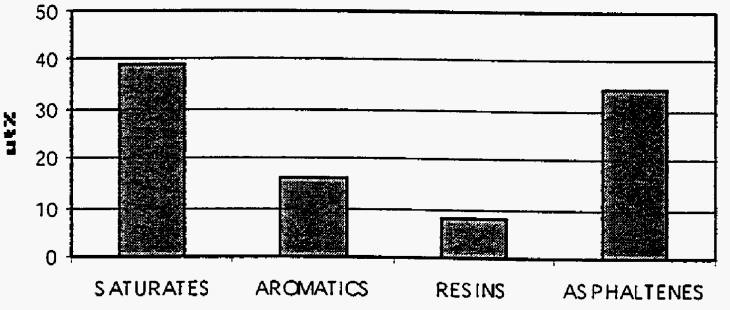

Figure 6:The SARA distribution of the precipitate obtained from one of the first-contact dead oil experiment

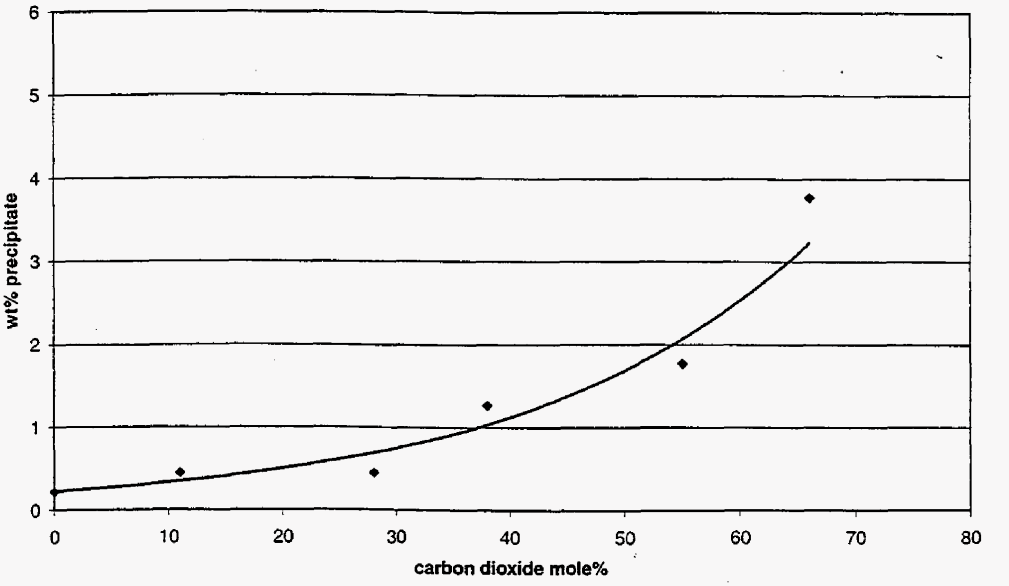

Figure 7 Weight percent precipitates obtained from live oil experiments

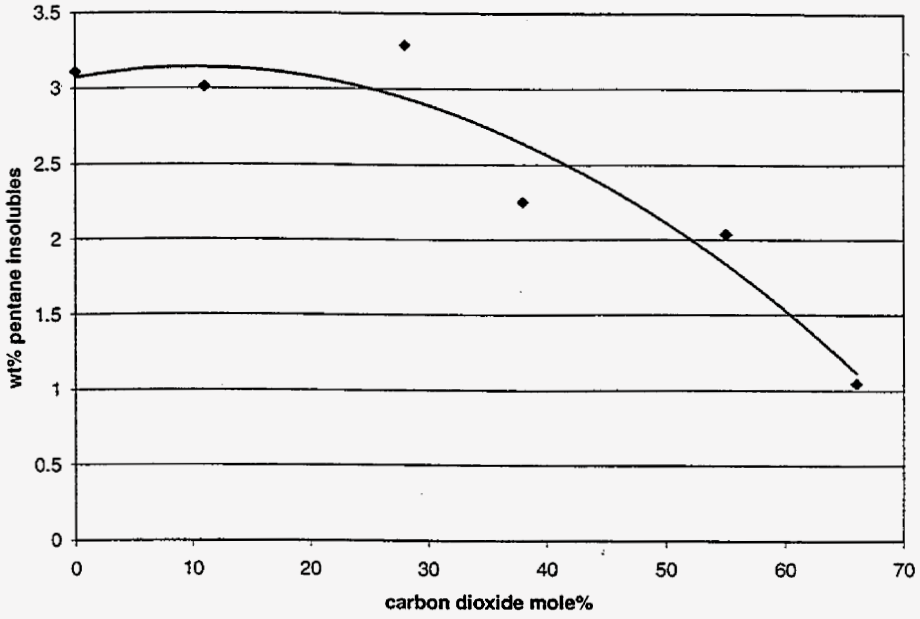

Figure 8: Weight percent asphaltenes in the oils from the live oil, first-contact experiments

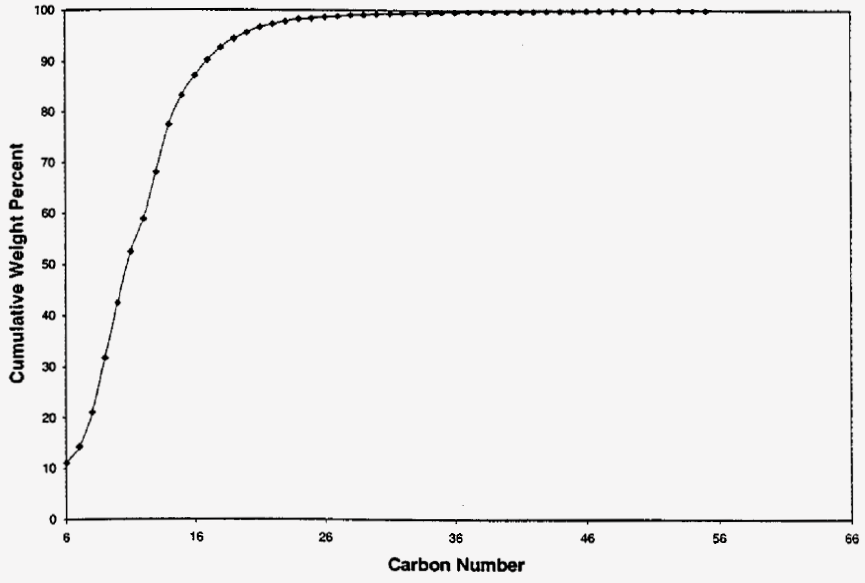

Figure 9: Cumulative carbon number distribution of the "light-cut" added to the oil to simulate forward multiple contacts

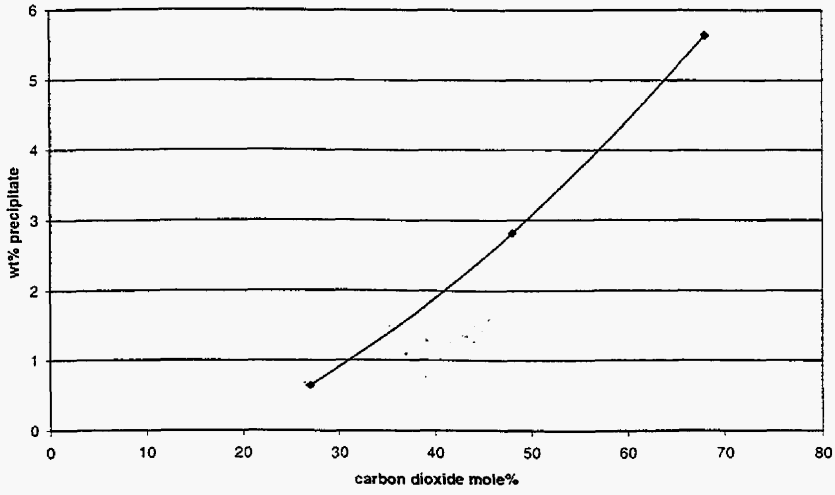

Figure 10: Amount of precipitate as a function of carbon dioxide concentration for the oil with light-cut added

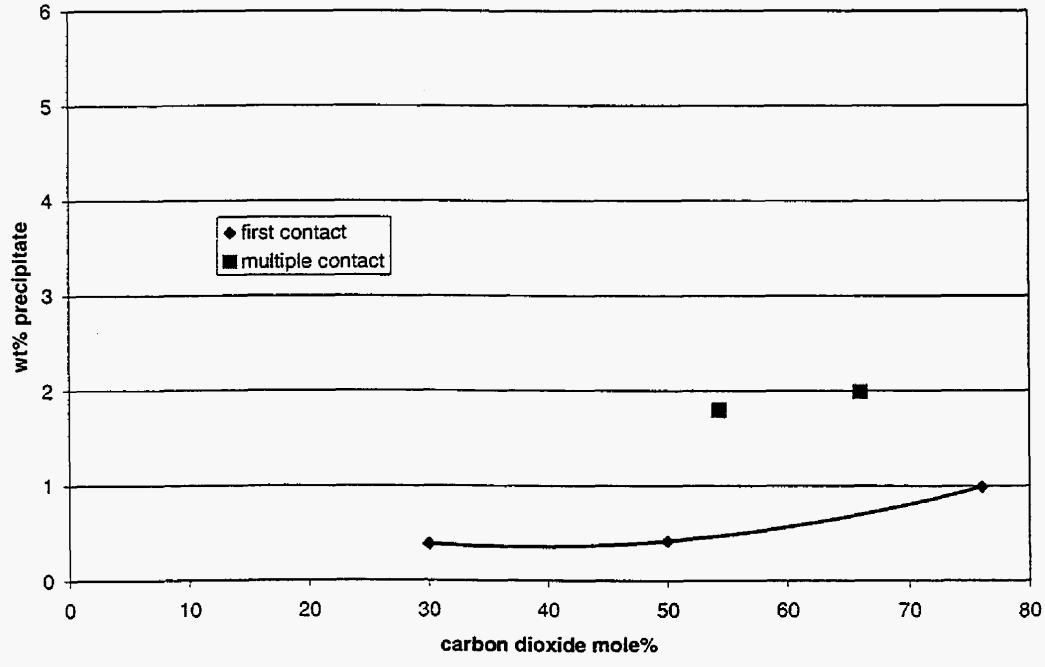

Figure 11: Comparison of the amount of carbon dioxide induced precipitation with the first and multiple contacts

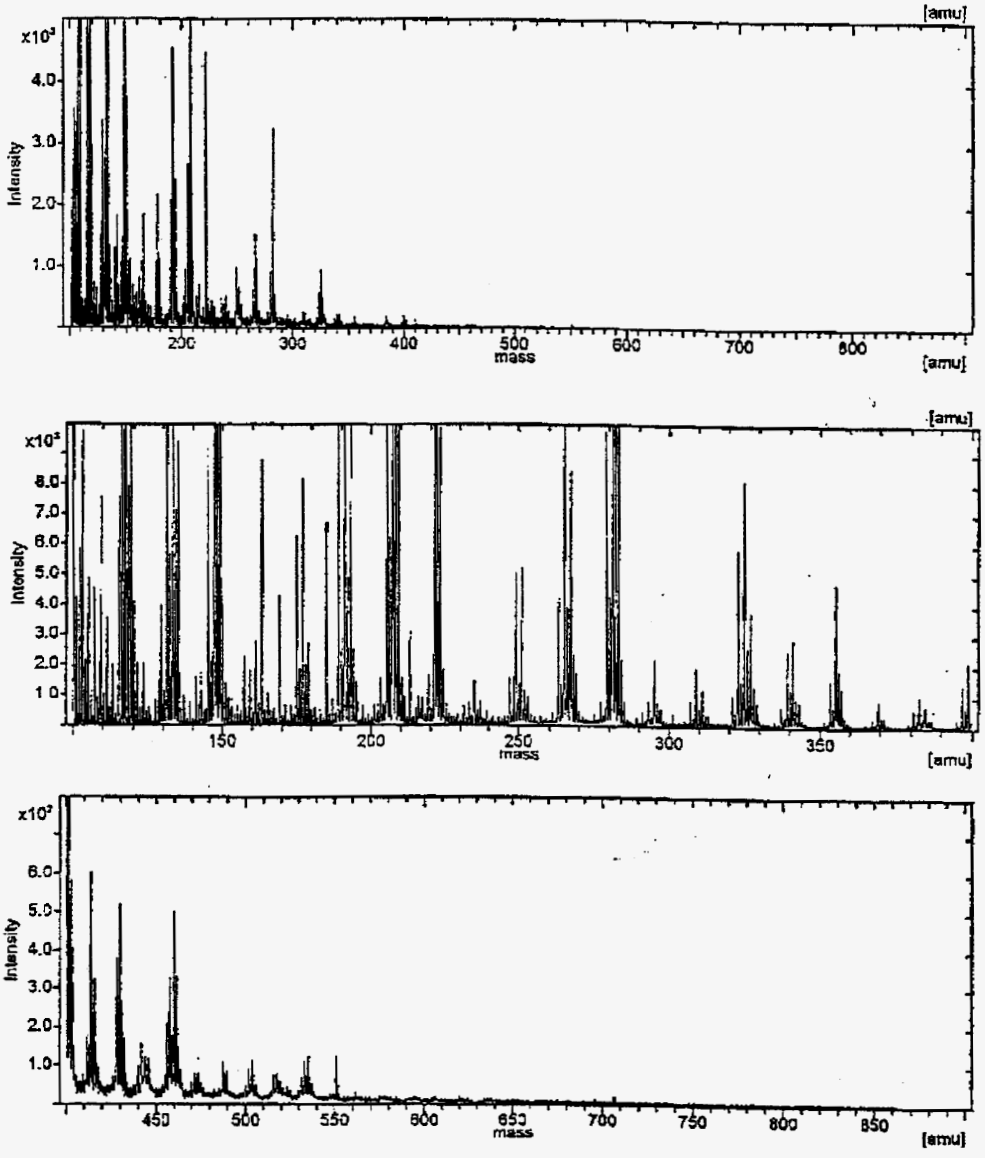

Figure 12: A positive ion TOF-SIMS(Time of Flight Mass Spectrometer) image of the asphaltenes from the field

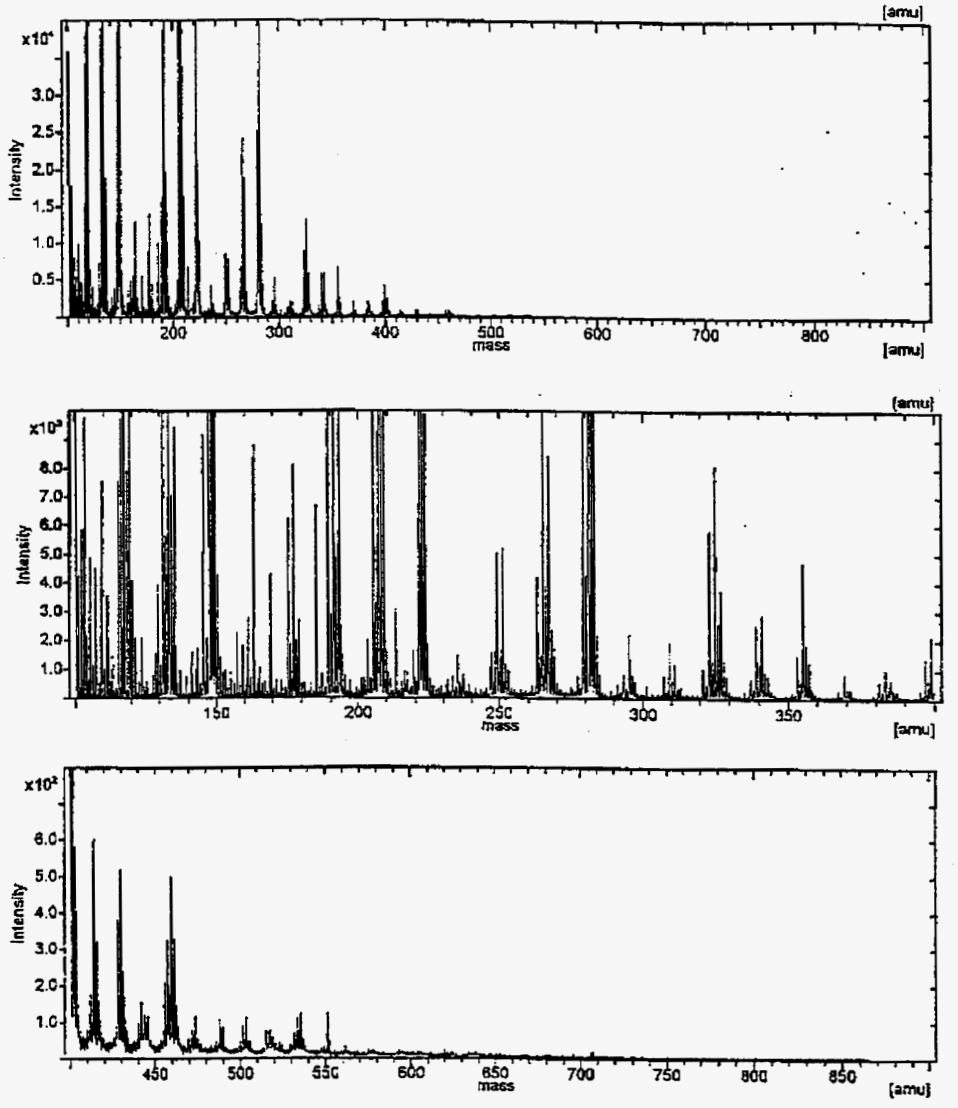

Figure 13: A positive ion TOF-SIMS (Time of Flight Mass Spectrometer) image of the solids obtained by contacting 50 mole% Phillips crude oil (oil from southern Utah) with 50% CO2

Thermodynamic Modeling of Asphaltene Precipitation

Introduction

Asphaltenes are polar polyaromatic, high molecular weight hydrocarbons and are amorphous in nature. Asphaltenes are insoluble in the low molecular weight normal paraffins and are classified by the type of precipitating paraffin since different paraffins precipitate different molecular weight ranges and hence different amounts of asphaltenes. Asphaltenes are commonly defined as n-heptane insoluble and benzene soluble fraction of crude oil following the Institute of Petroleum (IP) Method Test 143.

Resins are defined as the fraction of the crude oil not soluble in ethyl acetate but soluble in n-heptane, toluene, and benzene at room temperature. They are polycyclic aromatic compounds and are non-polar or neutral. Resins have a strong tendency to associate with asphaltenes. This reduces the aggregation of asphaltenes and determines their solubility in the crude oil. Because of the complexity of the nature of asphaltenes, the phenomena of asphaltene precipitation and flocculation are not well understood.

In this work, two molecular thermodynamic models of asphaltene precipitation are first reviewed. Also a fundamentally different thermodynamic model for wax precipitation is discussed. Some elements of both the models are combined and a new molecular thermodynamic model of asphaltene precipitation is presented.

Nature and Characteristics of Asphaltenes

The classic definition of asphaltenes is based on the solution properties of petroleum residuum in various solvents. This generalized concept has been extended to the low molecular weight n-paraffin insoluble and benzene soluble fraction derived from various carbonaceous sources, such as petroleum, coal and shale oil (Long, 1981). Asphaltenes must be classified by the particular precipitation solvent since different solvents cause different amounts of precipitation (Mitchell and Speight, 1973). In general, asphaltenes are classified as polar, aromatic high molecular weight hydrocarbons of amorphous structure and are believed to exist in crude oils partly in the form of colloidally dispersed fine particles and partly as dissolved compounds (Ferworn, 1995). The exact chemical structures of asphaltenic compounds is unknown and will depend on the type of crude oil; however, asphaltenes are believed to consist of aromatic ring structures with oxygen, nitrogen and sulphur present in heterocyclic side chains and oxygen in alkyl side chains.

Long (1981) proposed complete characterization of asphaltenes by considering molecular weight and molecular polarity as separate properties of the molecules. He demonstrated that asphaltenes contained a wide distribution of polarities and molecular weights.

Table 3 (Speight, 1991) shows elemental compositions of n-pentane asphaltenes. The elemental compositions of asphaltenes yield H/C ratios of 1.05~1.15 on a mole basis. The near constancy of this ratio is surprising when the number of possible molecular isomers of massive asphaltene molecules are considered. In contrast are the ratios of heteroatoms in crude oils, for example, oxygen 0.3~4.9%, nitrogen 0.6~3.3% and sulphur 0.3~10.3%.

In the petroleum reservoir, asphaltenes have been observed to occur as dissolved and as micelles or colloidal suspensions in the crude oil (Mansoori, 1988). Measurement of the surface tension indicates that there exists a critical micelle concentration (CMC) for dilute solutions of asphaltenes in toluene. With concentration below the CMC, the asphaltenes in the solution are in a molecular state, while above the CMC, associates and aggregates of asphaltenes may form. When resins and asphaltenes are both present as in petroleum, asphaltenes tend to associate with resins preferentially over association among themselves.

Mechanism of Asphaltene Deposition

It is important to accurately characterize and describe the mechanisms involved in asphaltene flocculation and precipitation for the development of realistic theoretical models. Asphaltene molecules are surrounded by resins that act as peptizing agents; that is, the resins maintain the asphaltenes in a colloidal dispersion (as opposed to a solution). The resins are typically composed of a highly polar end group, which often contains heteroatoms such as oxygen, sulphur and nitrogen, as well as long, non-polar paraffinic groups. The resins are attracted to the asphaltene micelles through their end group. This attraction is a result of hydrogen bonding through the heteroatoms and dipole-dipole interactions arising from the high polarities of the resin and asphaltene molecules. The paraffinic component of the resin molecule acts as a tail making the transition to the relatively non-polar bulk of the oil where individual molecules also exist in true solution. This equilibrium is disturbed when vastly differing molecules are introduced into the mixture. Normal alkane liquids (such as pentane or heptane) are often added to crude oils in an attempt to reduce heavy oil viscosities. The result of this introduction is an

alteration in the overall characteristics of the crude oil making it lighter. In response, resin molecules desorb from the surface of the asphaltenes in an attempt to re-establish the thermodynamic equilibrium that existed in the oil. This desorbtion of peptizing resins forces the asphaltene micelles to agglomerate in order to reduce their overall surface free energy. If sufficient quantities of the particular solvent are added to the oils, the asphaltene molecules aggregate to such an extent that the particles overcome the Brownian forces of suspension and begin to precipitate. It is obvious from this description that the quantity and type of solvent added to the crude oil is crucial to the amount and characteristics of the asphaltenes deposited.

In general, any action of chemical, mechanical or electrical nature which depeptizes the asphaltene micelles can lead to the precipitation of asphaltenes from the crude oil-asphaltene suspension.

Models for Prediction of Asphaltene (and Organic) Deposition

The liquid state of the petroleum is a result of a delicate balance between its constituents, which depend on each other for solubility. Deposition of asphaltene from petroleum crude due to the introduction of a solvent can be understood by the application of the principles of thermodynamics of multicomponent mixtures and phase equilibria. There are two types of models for asphaltene deposition: the solubility model; and the colloidal model. The basic principles of each of the asphaltene precipitation modeling approaches are discussed.

Thermodynamic Molecular Approach

The first important approach in modeling asphaltene precipitation in petroleum engineering is due to Hirschberg et al (1984). Burke et al (1990) also developed a similar model. Asphaltenes are considered as mono-dispersed polymeric molecules dissolved in the crude oil in this model. Therefore, it is called a homogeneous molecular thermodynamic model. This approach is based on the Flory-Huggins Polymer Theory. The crude oil is treated as a mixture of two liquid phases. The first phase is pure asphaltene liquid phase which acts as a solute and the second phase is the remaining components of the crude oil which acts as a solvent.

For simplicity, a combination of vapor/liquid and liquid/liquid model was used instead of a full three-phase model. Using a detailed compositional simulator based on SRK equation of state, liquid phase composition was calculated assuming no asphaltene precipitation. It was assumed that asphaltene precipitation would not disturb the vapor/liquid equilibrium. Then using the modified Flory-Huggins polymer solution theory, asphaltene precipitation from the liquid phase was calculated. Two pseudocomponents, asphalt and solvent were defined to describe the liquid as a quasi-binary mixture. The deasphalted crude or crude-solvent was treated as a single component. The composition of this component was calculated using the vapor/liquid equilibrium model. Using the solubility parameter and molar volume of the liquid phase, the solubility parameter and molar volume of the deasphalted liquid was calculated.

The effects of temperature and pressure were also considered in this model. In general, as pressure was increased, the solubility parameter of the solvent increased and the molar volume of the mixture decreased leading to an overall increase in asphaltene solubility. Below the bubble point pressure, the compression of the crude oil-solvent mixture was balanced against the dissolution of gas in the sample. The result of these competing forces was that asphaltene deposition was most severe at the bubble point pressure. Therefore, as the compressibility of the crude is the dominant factor in pressure-induced precipitation, its effect should occur predominantly in light crudes (which are candidates in CO_2 flooding) and condensates.

As the solubility parameter of asphaltene decreased with increasing temperature, the model predicted an increase in the solubility of asphaltene. However, at high temperatures, some dissociation appeared to occur between the asphaltene-resin complexes and this counteracted the increased solubility. This model was unable to quantitatively describe these phenomena.

The values of solubility parameter of asphaltenes were found to be fairly insensitive to the molar volume of asphaltenes. Hence amounts of asphaltenes precipitation in a mixture of tank oil and n-heptane was fitted with a molar volume of asphaltenes of 4.0 m^3/kmol and solubility parameter of 19.59 $Mpa^{0.5}$. The model showed fair agreement between experimental and theoretical values.

While the model has gained some general acceptance in the petroleum industry, its main drawback is the assumptions inherent in the development of the Flory-Huggins theory. The precipitated asphaltenes are considered as a liquid phase and therefore, the reference states of both the precipitated and dissolved asphaltenes are the same. This assumption reduces the effect of temperature on the system by ignoring the difference in standard state conditions.

Kawanaka et al (1991) extended Hirschberg's approach but used Scott-Magat theory to take into account the polydispersed nature of asphaltenes having a molecular weight distribution. This model is called heterogeneous or polydispersed molecular thermodynamic model. Unlike the homogeneous model, it was assumed that the properties of asphaltenes depended on their molecular weight. A continuous distribution function for asphaltenes molecular weight distribution was considered and using a continuous gamma distribution function, properties of asphaltenes were approximated with respect to their molecular weights. The experimental data on asphaltene precipitation due to addition of paraffinic hydrocarbons were used to optimize the adjustable parameters. The comparison between experimental and predicted asphaltene precipitation for various solvent/oil ratios showed good match for solvent/oil ratios ranging from 2.22 to 50 cm^3 solvent/g tank oil.

The model allowed the calculation of the distributions of asphaltenes in the solvent-rich liquid phase, in the solid phase and in the original crude. The model was used to predict the phase behavior and precipitation region of asphaltenes in CO_2-crude oil mixtures at different pressures and compositions of the injection fluid. Precipitation, however, occurred only at high CO_2 concentrations (~90%).

Nghiem and coworkers (1993, 1996) proposed a different molecular thermodynamic model. In their model, the precipitated asphaltenes were modeled as pure dense phase. This phase was referred to as asphalt phase and can either be a liquid or a solid. One of the important contributions of this model was characterizing the asphaltene component. Previous approaches assumed that asphaltene was the heaviest component in the oil. In this model, the heaviest component was split into two components: a non-precipitating component and a precipitating component. These two components have identical critical properties and acentric factors, but their interaction coefficients with the light components are different. The precipitating component has larger interaction coefficients

with the light components. Larger interaction coefficients correspond to greater "incompatibility" between components and favor the formation of the asphalt phase. The non-precipitating component can be related to resins, asphaltene/resin micelles that will not dissociate, and heavy paraffins. The precipitating component corresponds to both the asphaltenes that could dissociate and precipitate and to the asphaltene/resin micelles that precipitate unaltered. A robust flash calculation procedure for vapor/liquid/asphalt systems was described. The model was tested using data from the literature and the industry. However, it seemed not suitable for other data.

Thermodynamic Colloidal Approach

A thermodynamic colloidal model has been developed by Leontaritis (1989). This approach assumed that asphaltenes exist in the oil in colloidal suspension, stabilized by resins adsorbed on their surface. This model was capable of predicting the onset of flocculation of colloidal asphaltenes in oil mixture induced by flow or generation of streaming potential due to flow of asphaltenes containing oil in conduits or porous media.

The chemistry and mathematics of colloidal suspensions were used in the development of this model. By assuming that the original system is composed of asphaltene molecules (colloids, with their surface covered by resin molecules), that are suspended in crude oil, it is possible for colloids to agglomerate under static or dynamic conditions. For asphaltene precipitation under static conditions, there must be a change in the system temperature, pressure or composition; that is, this portion of the model is thermodynamic based. Should the resin concentration decrease below some critical value, the asphaltenes will agglomerate to reach a lower overall energy state and then precipitate. This critical value is found by calculating the critical resin chemical potential from resin solubility and volumetric data obtained in an experimental determination of the onset of asphaltene deposition. This critical value may be compared to electric potentials calculated at reservoir and/or processing conditions to determine if deposition would occur. If the calculated potential at reservoir conditions is less than the critical value, deposition will occur.

As the asphaltene molecules are highly polar, the flow of an oil containing these charged particles initiates a streaming potential. For experimental or typical industry production conditions, the streaming potential necessary for asphaltene deposition in a

pipe or well maybe calculated. If this streaming potential exceeds that which exists in the practical system, deposition should occur.

This model is capable of predicting the conditions where asphaltene deposition should occur. However, it is not possible to determine the extent of asphaltene deposition with either the static or dynamic conditions.

Wax Formation Approach

Won (1985, 1986 and 1989) developed a wax model based on liquid-solid equilibrium (LSE) approach in 1985. Based on Scatchard-Hildebrand regular solution theory, an equation for a solid-liquid equilibrium constant was developed by equating the fugacities of components in the solid and liquid phases. The standard state fugacities of the liquid and solid phase components are determined by calculating the Gibbs free energy change of component from liquid to solid. In this model, every component may enter into the solid phase depending on its fusion temperature, fusion enthalpy and solubility parameters in liquid phase and the solid phase. Hence, estimating these values is very important. Recently, some attempts (Pedersen, 1991; Hansen, 1988 and Lira-Galena and Firoozabadi, 1996) were made for improved estimation of fusion temperature, fusion enthalpy and solubility parameters.

Model Development and Theory

Homogeneous Molecular Thermodynamic Model

This approach is based on the Flory-Huggins polymer solution theory. The crude oil is treated as a mixture of two liquid phases. The first phase is pure asphaltene liquid phase which acts as a solute and the second phase consists of the remaining components of the crude oil which acts as a solvent. The asphaltene volume fraction of the soluble in the crude is given by the following equation:

$$\phi_A = \exp\left(\frac{V_A}{V_L}\left(1-\frac{V_L}{V_A}-\frac{V_L}{RT}(\delta_A-\delta_L)^2\right)\right)$$

Therefore, the difference between the maximum amount (in weight fraction) of asphaltene W_m that is measured in an experiment and what is predicted by the above equation yields the amount of the precipitated solid.

$$W_A = (W_m - \phi_A) \times 100\%$$

The molar volume (V_A) and solubility parameter (δ_A) of the asphaltene fraction are evaluated by fitting the model with the experimental data. The molar volume (V_L) and solubility parameter of liquid phase (δ_L) is calculated from the Peng-Robinson equation of state (EOS).

The polynomial form of Peng-Robinson EOS is given by the following equation:

$$Z^3 - (1-B)Z^2 + (A - 3B^2 - B)Z - (AB - B^2 - B^3) = 0$$

Where

$$A = \frac{a_L P}{(RT)^2} \qquad B = \frac{b_L P}{RT}$$

Parameters a_L and b_L are determined as follows:

$$a_L = \sum_i \sum_j x_i x_j a_{ij}$$

$$a_{ij} = (1 - \sigma_{ij})\sqrt{a_i a_j}$$

$$a_i = 0.45724 \frac{R^2 {Tc_i}^2}{{Pc_i}^2} \alpha_i$$

$$\alpha_i = 1 + (0.37464 + 1.54226\omega_i - 0.26992{\omega_i}^2)(1 - \sqrt{\frac{Tc_i}{T}})$$

And

$$b_L = \sum_i x_i b_i$$

$$b_i = 0.0778 \frac{RTc_i}{Pc_i}$$

Z_L is first calculated by solving the cubic equation; then V_L is calculated by:

$$V_L = \frac{Z_L RT}{P}$$

In regular solution theory, the solubility parameter is defined as:

$$\delta_L = \left(\frac{\Delta U_L{}^V}{V_L} \right)^{1/2}$$

In order to develop an expression for this parameter we start with the expression for the internal energy of a fluid.

$$dU = TdS - PdV$$

Dividing each term by dV and substituting the Maxwell relation $(\partial S/\partial V)_T=(\partial P/\partial T)_v$ yields:

$$\left.\frac{\partial U}{\partial V}\right|_T = T\left.\frac{\partial P}{\partial T}\right|_V - P$$

Taking the pressure derivative of the Peng-Robinson equation with respect to temperature at constant volume,

$$\left.\frac{\partial U}{\partial V}\right|_T = \frac{a_L - T\dfrac{da_L}{dT}}{\left(V_L + b_L\left(\sqrt{2}+1\right)\right)\left(V_L - b_L\left(\sqrt{2}-1\right)\right)}$$

Integrating the above equation by parts,

$$\Delta U_L{}^V = \left(\frac{a_L - T\dfrac{da_L}{dT}}{2\sqrt{2}b_L} \right) \ln\left(\frac{V_L + (1+\sqrt{2})b_L}{V_L + (1-\sqrt{2})b_L} \right)$$

Then

$$\delta_L{}^2 = \left(\frac{a_L - T\dfrac{da_L}{dT}}{2\sqrt{2}b_L V_L} \right) \ln\left(\frac{V_L + (1+\sqrt{2})b_L}{V_L + (1-\sqrt{2})b_L} \right)$$

Where

$$\frac{da_L}{dT} = \sum_i \sum_j \left(x_i x_j (1-\sigma_{ij}) (a_i a_j Tc_i Tc_j)^{1/2} \left[1 + K_j \left(1 - \sqrt{Tr_j} \right) \right] \left(-0.5 K_i \sqrt{Tr_i} \right) + \right.$$

$$\left. \left[1 + K_i \left(1 - \sqrt{Tr_i} \right) \right] \left(-0.5 K_j \sqrt{Tr_j} \right) \right)$$

$$Tr_i = \frac{T}{Tc_i} \qquad K_i = 0.37464 + 1..54226\omega_i - 0.26992\omega_i{}^2$$

The calculation procedure using the homogeneous thermodynamic model is shown in a block diagram in Figure 14.

Polydispersed Molecular Thermodynamic Model

This approach is based on the Scott-Magat theory to represent solid-liquid equilibria for various asphaltene fractions. A normal distribution function is used to represent asphaltene molecular weight distribution in the crude oil. The solubility parameters and other properties of each asphaltene of the components are calculated using the average molecular weights of each asphaltene pseudo-component from critical property correlation proposed by Twu (1984) and Gambill (1957).

Discretization of Normal Distribution Function

A continuous normal distribution function of the molecular weight $F(M_A)$ of the asphaltene fraction is given by:

$$F(M_{Ai}) = \frac{1}{\sigma\sqrt{2\pi}} \exp\left(-\zeta_i{}^2 / 2 \right)$$

Where

$$\zeta_i = \frac{M_{Ai} - \overline{M}_A}{\sigma}$$

Here, M_{Ai} is the molecular weight of ith asphaltene component, $\overline{M}_A$ is the average molecular weight of all asphaltene components and σ is standard deviation of the normal distribution function. For practical purpose, it is sufficient to approximate the span of molecular weights to 6σ since it causes only 0.26% error in calculation. If we have N_A pseudo-components in the asphaltenic portion of the oil, then

$$\Delta M_A = \frac{6\sigma}{N_A}$$

With the initial molecular weight M_{Ao}, the molecular weight of ith component of asphaltene M_{Ai} is given by:

$$M_{Ai} = M_{Ao} + \frac{3\sigma}{N_A}(2i-1)$$

We also know

$$\overline{M}_A = M_{Ao} + 3\sigma$$

Then

$$\zeta_i = \frac{M_{Ai} - \overline{M}_A}{\sigma} = \frac{3}{N_A}(2i-1-N_A)$$

If $\overline{M}_A$ and σ are known, we can obtain M_{Ai} by:

$$M_{Ai} = \overline{M}_A + \sigma\zeta_i = \overline{M}_A + \frac{3\sigma}{N_A}(2i-1-N_A)$$

Now we introduce the model parameter β which is the ratio of total mole fraction of asphaltenes to the mole fraction of plus fraction. If X_{AT} is the total mole fraction of asphaltenes in the liquid phase, then:

$$X_{AT} = \beta X_{+}$$

$$X_{Ai} = \frac{3\sqrt{2}X_{AT}}{\sqrt{\pi}N_A}\exp(-0.5\zeta_i)^2$$

If there are NF asphaltene free components, then

$$X_{NF} = X_{+} - X_{AT} = X_{+}(1-\beta)$$

$$M_{NF} = \frac{M_{+}X_{+} - \overline{M}_A X_{AT}}{X_{NF}}$$

Molar Properties

The molar volume and solubility parameter of solvent-oil mixture are calculated using the same procedure as the homogeneous model.

The molar volume of each asphaltene component is given by:

$$V_{Ai} = V_{Ai}^{Lmix} = V_{Ai}^{L} = V_{Ai}^{S} = \frac{M_{Ai}^{Lmix}}{\rho_A}$$

where ρ_A is the average density of asphaltenes. The average molecular weight of asphaltene-free components in the Lmix phase is given by:

$$\overline{M}_B^{Lmix} = \sum_{j=1}^{NF} M_j^{Lmix} X_j^{Lmix}$$

The interaction parameter K_{AB} is treated as a linear function of the molecular weight:

$$K_{AB} = a' + b'\overline{M}_B{}^{Lmix}$$

Where a′ and b′ are two model parameters obtained by fitting experimental asphaltene precipitation data. This interaction parameter allows for representing the effect of solvent/oil ratio and solvent molecular ratio in this model.

The normal boiling point of asphaltene component T_{bi} is obtained from the following equation:

$$T_{bi} = \exp\left(5.71419 + 2.71579\theta_i - 0.28659\theta_i{}^2 - \frac{39.8544}{\theta_i} - \frac{0.122488}{\theta_i{}^2}\right)$$

$$-24.7522\theta_i + 35.315\theta_i{}^2$$

Where

$$\theta_i = \ln\left(M_{Ai}{}^{Lmix}\right)$$

The reference critical temperature, T_{Ci}° is given by:

$$T_{Ci}{}^{o} = {}^{T_{bi}}\Big/\left(0.533272 + 0.000191017T_{bi} + 0.779681\times10^{-7}T_{bi}{}^2 - 0.284376\times10^{-10}T_{bi}{}^3\right)$$

The reference temperature T_{Ci} is obtained by:

$$T_{Ci} = T_{Ci}{}^{o}\left(\frac{1+2f_T^i}{1-2f_T^i}\right)^2$$

Where

$$f_T^i = \Delta SG_T^i\left(\frac{-0.352456}{\sqrt{T_{bi}}} + \Delta SG_T^i\left(0.0398285 - \frac{0.948125}{\sqrt{T_{bi}}}\right)\right)$$

And

$$\Delta SG_T^i = \exp\left(5\left(SG_i^o - SG_i\right)\right) - 1$$

The reference specific gravity SG_i^o and specific gravity SG_i are given by:

$$SG_i^o = 0.843593 - 0.128624\alpha_i - 3.36159\alpha_i^3 - 13749.5\alpha_i^{12}$$

$$SG_i = 6.0108 M_{Ai}^{0.13541} v^{-1.18241}$$

Where

$$\alpha_i = 1 - \frac{T_{bi}}{T_{Ci}^o}$$

$$v = \left(\frac{0.16637 SG_+ S_o}{Z_+ M_+} \right)^{-0.84573}$$

$$SG_+ = \frac{\rho_+}{62.4}$$

$$S_o = \sum_{i=1}^{N_A} X_{Ai}^{Lmix} M_{Ai}^{0.86459}$$

$$Z_+ = \sum_{i=1}^{N_A} X_{Ai}^{Lmix}$$

Where ρ_+ is the average density of the plus fraction prior to splitting. The heat of vaporization for each asphaltene component is given by:

$$\Delta H_i^T = 1.014\left[T_{bi}\left(8.75+4.571\log_{10}(T_{bi})\right)\right]\left(\frac{T_{Ci}-T}{T_{Ci}-T_{bi}}\right)^{0.38}$$

The solubility parameter for each asphaltene component is given by:

$$\delta_{Ai} = \left(\frac{\Delta H_i^T - RT}{V_{Ai}^{Lmix}}\right)^{0.5}$$

The volume fraction of each asphaltene component in the Lmix phase is obtained by:

$$\phi_{Ai}^{Lmix} = \frac{X_{Ai}^{Lmix} V_{Ai}^{Lmix}}{V_{Lmix}}$$

and the volume fraction of asphaltene-free components in the Lmix phase

$$\phi_B{}^{Lmix} = 1 - \sum_{i=1}^{N_A} \phi_{Ai}^{Lmix}$$

The average solubility parameter for asphaltenes and asphaltene free liquid are then obtained.

$$\delta_A = \frac{\sum_{i=1}^{N_A} \phi_{Ai}^{Lmix}\delta_{Ai}}{1-\phi_B}$$

$$\delta_B = \frac{\delta_{Lmix} - \delta_A(1-\phi_B)}{\phi_B}$$

The molar volumes of the asphaltene fraction and asphaltene free liquid are obtained:

$$V_A = \frac{\sum_{i=1}^{N_A} V_{Ai}^{Lmix} X_{Ai}^{Lmix}}{X_{AT}^{Lmix}}$$

$$V_B = \frac{V_{Lmix} - \sum_{i=1}^{N_A} V_{Ai}^{Lmix} X_{Ai}^{Lmix}}{1 - X_{AT}^{Lmix}}$$

Scott-Magat Theory

Scott-Magat theory is expressed by the following equation:

$$\frac{\mu_{Ai} - \mu_{Ai}^{o}}{RT} = \ln \phi_{Ai} + 1 - \frac{m_{Ai}}{\overline{m}_A}(1 - \phi_B) - m_{Ai}\phi_B + f m_{Ai}\phi_B^{\,2}$$

μ_{Ai} and μ_{Ai}° are respectively the chemical potential and standard chemical potential of the ith pseudo-component of asphaltene in a mixture of asphaltene and solvent. Subscripts A_i and B refer to the ith component of asphaltene and asphaltene-free liquid phase. The term ϕ_{Ai} is the volume fraction of the ith component of asphaltene and ϕ_B is the volume fraction of asphaltene-free liquid phase. The term m_{Ai} is the segment number of the ith component of asphaltene which is defined as:

$$m_{Ai} = \frac{V_{Ai}}{V_B}$$

$\overline{m}_A$ is the average segment number of asphaltene which is defined as:

$$\overline{m}_A = \sum_{i=1}^{N_A} \frac{X_{Ai}}{X_{AT}} m_{Ai} = \frac{V_A}{V_B}$$

The parameter f is defined as:

$$f = \frac{1}{r} + \frac{V_B\left[(\delta_A - \delta_B)^2 + 2K_{AB}\delta_A\delta_B\right]}{RT}$$

The parameter f consists of two parts: a term 1/r resulting from entropy of mixing and the second term resulting from the heat of mixing. Other parameters involved in this equation have been defined previously.

Considering $V_{Ai}^{S}=V_{Ai}^{L}=V_{Ai}$, $V_B^{S}=V_B^{L}=V_B$, $m_{Ai}^{S}=m_{Ai}^{L}=m_{Ai}$, $\overline{m}_A^{S}=\overline{m}_A^{L}=\overline{m}_A$ and $\phi_B^{S}=0$, for the ith asphaltene component in the equilibrium solid phase, we have:

$$\frac{\mu_{Ai}^{S}-\mu_{Ai}^{o}}{RT} = \ln\phi_{Ai}^{S} + 1 - \frac{m_{Ai}}{\overline{m}_A}$$

For the ith asphaltene component in the equilibrium liquid phase, we have:

$$\frac{\mu_{Ai}^{L}-\mu_{Ai}^{o}}{RT} = \ln\phi_{Ai}^{L} + 1 - \frac{m_{Ai}}{\overline{m}_A}(1-\phi_B) - m_{Ai}\phi_B + fm_{Ai}\phi_B^2$$

Equating the chemical potentials of each asphaltene component in the equilibrium solid and liquid phase,

$$\mu_{Ai}^{S} - \mu_{Ai}^{L} = 0$$

We have:

$$\ln\left(\frac{\phi_{Ai}^{S}}{\phi_{Ai}^{L}}\right) - \frac{m_{Ai}}{\overline{m}_A}\phi_B + m_{Ai}\phi_B - fm_{Ai}\phi_B^2 = 0$$

$$\ln\left(\frac{\phi_{Ai}^{S}}{\phi_{Ai}^{L}}\right) = m_{Ai}\left[\phi_B\left(\frac{1}{\overline{m}_A}-1\right) + f\phi_B^2\right]$$

Then,

$$\ln\left(\frac{\phi_{Ai}^{S}}{\phi_{Ai}^{L}}\right)=\frac{V_{Ai}}{V_B}\left[\phi_B\left(\frac{V_B}{V_A}-1\right)+f\phi_B^2\right]$$

Finally, the equilibrium constant for the ith component of asphaltene K_{Ai} is obtained by:

$$K_{Ai}=\frac{\phi_{Ai}^{S}}{\phi_{Ai}^{L}}=\exp\left[\phi_B\left(\frac{V_{Ai}}{V_A}-\frac{V_{Ai}}{V_B}\right)+f\frac{V_{Ai}}{V_B}\phi_B^2\right]$$

Equilibrium Composition of Precipitated Asphaltenes

It is assumed that

$$V_A^{Lmix}=V_A^{L}=V_A$$
$$V_B^{Lmix}=V_B^{L}=V_B$$

By considering the material balance for each asphaltene component between Lmix, L and S phases we can obtain an expression to calculate the mole fractions of asphaltenes in the L phase.

$$X_{Ai}^{L}=\frac{X_{Ai}^{Lmix}}{\left(\frac{V_{Lmix}-V_A}{V_L-V_A}\right)+K_{Ai}\frac{V_A}{V_L}\left(\frac{V_L-V_{Lmix}}{V_L-V_A}\right)}$$

V_L is obtained by Newton Raphson iteration technique. Since $V_{Ai}^{S}=V_{Ai}^{L}=V_{Ai}$ and $V_A=V_A^{L}$, then

$$V_A=\sum_{i=1}^{N_A}V_{Ai}X_{Ai}^{L}$$

$$f(V_L) = V_A - \sum_{i=1}^{N_A} \frac{V_{Ai} X_{Ai}^{Lmix}}{\left(\frac{V_{Lmix} - V_A}{V_L - V_A}\right) + K_{Ai} \frac{V_A}{V_L}\left(\frac{V_L - V_{Lmix}}{V_L - V_A}\right)} = 0$$

V_L(new) is calculated by:

$$V_L(new) = V_L(old) - \frac{f(V_L)}{f'(V_L)}$$

Now we can calculate the precipitated asphaltene solid by the following equation:

$$W_{AD} = \left(\frac{V_L - V_{Lmix}}{V_L - V_A}\right) \frac{X_{AT}^{TO}}{X_{AT}^{Lmix}} \frac{\overline{M}_S}{\overline{M}_{TO}}$$

Where W_{AD} is the calculated weight fraction of deposited asphaltene, X_{AT}^{TO} is the total mole fraction of asphaltenes in the tank oil, X_{AT}^{Lmix} is the total mole fraction of asphaltenes in the Lmix phase, $\overline{M}_{TO}$ is the average molecular weight of tank oil and $\overline{M}_S$ is the average molecular weight of solid phase. Here

$$\overline{M}_S = \sum_{i=1}^{N_A} M_{Ai} X_{Ai}^S = \sum_{i=1}^{N_A} M_{Ai} K_{Ai} X_{Ai}^L \frac{V_A}{V_L}$$

In this model, we have five parameters totally. They are average asphaltene molecular weight $\overline{M}_A$, ratio of total mole fraction of asphaltene to the mole fraction of plus fraction β, standard deviation of the asphaltene molecular weight distribution σ, and constants of the asphaltene and asphaltene-free crude oil interaction equations a' and b'. These parameters are obtained by fitting the experimental data. Once the model parameters are known, the model can be used to predict asphaltene precipitation amount under other conditions. The flow diagram of calculations using the polydispersed model is shown in Figure 15.

Wax Formation Model

At thermodynamic equilibrium, the fugacity of component i in liquid phase must be equal to the fugacity in the solid phase.

$$f_i^L = f_i^S$$

$$f_i^L = \gamma_i^L x_i^L f_i^{\circ L} \exp\left(\int_0^P \frac{V_i^L dP}{RT}\right)$$

$$f_i^S = \gamma_i^S x_i^S f_i^{\circ S} \exp\left(\int_0^P \frac{V_i^S dP}{RT}\right)$$

$$\frac{x_i^S}{x_i^L} = \frac{\gamma_i^L f_i^{\circ L}}{\gamma_i^S f_i^{\circ S}} \exp\left(\int_0^P \frac{(V_i^L - V_i^S)dP}{RT}\right)$$

If V_i^L, $V_i^S \neq f(P)$, then

$$\frac{x_i^S}{x_i^L} = \frac{\gamma_i^L f_i^{\circ L}}{\gamma_i^S f_i^{\circ S}} \exp\left(\frac{V_i^L - V_i^S}{RT} P\right)$$

At low to moderate pressure, the concentration associated with the liquid-wax transition must be expected not to exceed 10%. Volume difference of this order of magnitude will have little influence on the liquid-wax equilibrium because the exponential term will be close to unity.

$$\frac{x_i^S}{x_i^L} = \frac{\gamma_i^L f_i^{\circ L}}{\gamma_i^S f_i^{\circ S}}$$

Meanwhile,

$$\Delta G^i = RT \ln\left(\frac{f_i^{\circ S}}{f_i^{\circ L}}\right)$$

$$\Delta G = \Delta H - T\Delta S$$

$$\Delta H = -\Delta H^f + \int_T^{T^f} (C_p^L - C_p^S) dT$$

$$\Delta S = -\frac{\Delta H^f}{T^f} + \int_T^{T^f} \left(\frac{C_p^L - C_p^S}{T}\right) dT$$

It is assumed that the heat capacities in S and L are equal, then

$$\frac{f_i^{\circ L}}{f_i^{\circ S}} = \exp\left(\frac{\Delta H_i^f}{RT}\left(1 - \frac{T}{T_i^f}\right)\right)$$

$$\frac{x_i^S}{x_i^L} = \frac{\gamma_i^L}{\gamma_i^S} \exp\left(\frac{\Delta H_i^f}{RT}\left(1 - \frac{T}{T_i^f}\right)\right)$$

Calculating the activity coefficients from the solubility parameters based on the regular solution theory.

$$\ln \gamma_i^L = \frac{V_i^L (\delta_i^L - \bar{\delta}^L)^2}{RT}$$

$$\ln \gamma_i^S = \frac{V_i^S (\delta_i^S - \bar{\delta}^S)^2}{RT}$$

Where,

$$\bar{\delta}^L = \sum_i \Phi_i^L \delta_i^L$$

$$\bar{\delta}^S = \sum_i \Phi_i^S \delta_i^S$$

$$\Phi_i^L = \frac{x_i^L V_i^L}{\sum_i x_i^L V_i^L}$$

$$\Phi_i^S = \frac{x_i^S V_i^S}{\sum_i x_i^S V_i^S}$$

Finally,

$$K_i = \frac{x_i^S}{x_i^L} = \exp\left(\frac{\Delta H_i^f}{RT}\left(1 - \frac{T}{T_i^f}\right) + \frac{V_i}{RT}\left(\left(\delta_i^L - \bar{\delta}^L\right)^2 - \left(\delta_i^S - \bar{\delta}^S\right)^2\right)\right)$$

Material balance in solid and liquid phases.

$$L + S = 1.0$$

$$x_i^F = L x_i^L + S x_i^S = (1-S) x_i^L + S x_i^S$$

$$x_i^L = \frac{x_i^F}{1 + S(K_i - 1)}$$

$$x_i^S = \frac{x_i^F K_i}{1 + S(K_i - 1)}$$

$$K_i = \frac{x_i^S}{x_i^L}$$

Then,

$$\sum_i x_i^L = \sum_i \frac{x_i^F}{1+S(K_i-1)} = 1$$

$$\sum_i x_i^S = \sum_i \frac{x_i^F K_i}{1+S(K_i-1)} = 1$$

$$F = \sum_i x_i^L - \sum_i x_i^S = \sum_i \frac{x_i^F (K_i-1)}{1+S(K_i-1)} = 0$$

Using Newton iteration method,

$$S_{j+1} = S_j - \frac{F(S_j)}{(\frac{dF}{dS})_{S_j}}$$

$$(\frac{dF}{dS})_{S_j} = -\sum_i \frac{x_i^F (K_i-1)^2}{(1+S_j(K_i-1))^2}$$

With initial guess S=0.5, γ_i^L=1.0, γ_i^S=1.0, we can calculate x_i^L, x_i^S and K_i, then repeat this procedure until convergence (S_{j+1}-S_j<0.001) obtained.

Extended Polydispersed Molecular Thermodynamic Model

In polydispersed molecular thermodynamic model, a continuous distribution function for asphaltene molecular weight distribution is considered. Using this distribution function, properties of asphaltenes are approximated with respect to their molecular weight. It is assumed that precipitated asphaltenes are from the plus fraction only and the range of asphaltene molecular weight is usually 1000~2000. However, in our experiments, the compounds with molecular weights as low as 300 have been found. This makes it

necessary to consider components lighter than plus fraction to form the deposition. On the other hand, we know that every component may enter into the solid phase in the wax model. So, we combine polydispersed model and the wax precipitation model to obtain an extended polydispersd molecular thermodynamic model.

In this model, we assume that any component will potentially be in the solid phase if its molecular weight is above 300. If there are N_p components in the oil-solvent mixture which can form deposition besides the N_A asphaltene components from the plus fraction, we have N_{AT} asphaltene components totally.

$$N_{AT} = N_A + N_P$$

In the polydispersed model, we introduce the parameter β to represent the mole fraction of asphaltene from the plus fraction. Now we can do the same thing to N_p components of the oil-solvent mixture. If the parameter η is used to represent the ratio of the mole fraction of asphaltene among N_p components, the molar fraction of asphaltene for the ith component among N_p components is obtained by the following equation :

$$X^i_{AT} = i\eta X^i_{Lmix} \qquad i = 1, N_P$$

The molar properties of N_p asphaltene components are calculated using correlations provided by Twu (1984) and Gambill (1957). The new parameter η is obtained by fitting some experimental data.

Results and Discussion

Homogeneous Molecular Thermodynamic Model

This Model has two parameters, molar volume and solubility parameter of asphaltenes. After model parameters are fitted by experimental data, it can be used to predict the precipitation amount of asphaltenes from the solvent-oil mixture.

To illustrate the application of this model for the asphaltene-deposition predictions, the data of Hirschberg (1984) tank oil are used. Table 4 shows the data for this tank oil. For initial guesses of the parameters, literature values are used. The maximum amount asphaltene W_m in the crude oil is assumed to be 0.1. For different solvent-oil mixtures,

the two parameters are optimized separately. The optimized values of parameters are shown in Table 5 . Table 6 gives the comparison of experimental and predicted amounts of asphaltene precipitation for various solvents. A good match can be seen between the experimental and predicted amounts of asphaltene precipitation.

One limitation of this model is that parameters fitted with experimental data at low pressure are not useful in predicting asphaltene precipitation at higher pressure since the molar properties of liquid phase will change with the pressure.

Polydispersed Molecular Thermodynamic Model

In this model, asphaltenes are considered as heterogeneous molecules with the normal distribution of molecule weight. We have five parameters totally. They are average asphaltene molecular weight $\overline{M}_A$, ratio of total mole fraction of asphaltene to the mole fraction of plus fraction β, standard deviation of the asphaltene molecular weight distribution σ, and constants of the asphaltene and asphaltene-free crude oil interaction equation a' and b'. With the knowledge of these model parameters, the model can be used to predict asphaltene precipitation amount under other conditions.

To test the validation of this model, the data of Hirschberg (1984) tank oil are used. The optimized model parameters for various solvents are given in Table 7. Table 8 shows the comparison of experiment and predicted amounts of asphaltene precipitation for various solvents at various dilution ratios.. For hexane, we use the average model values of n-pentane and n-heptane to predict asphaltene precipitation amount due to the lack of experimental data. The parameter β decreases but the parameter σ increases along with the increase of carbon number of solvents. It is evident that with increase in the dilution ratio, the asphaltene precipitation initially increases till a certain limit and then it levels off. A match better than the homogeneous thermodynamic molecular model can be seen between the experimental and predicted amounts of asphaltene precipitation. We can also see that the onset of deposition, that is, the critical ratio at which precipitation starts increases along with the increase of the carbon number of the solvents.

In our laboratory, asphaltene precipitation of Rangely oil is being investigated. The composition data of tank oil obtained by gas chromatography (simulated distillation) is given in Table 9. We represent it by eight pseudo-components using the method of CMG Winprop (1999). First the plus fraction C60+ is split into 10 components, then 69

components are lumped into eight pseudo-components. Table 10 gives molar fraction and thermodynamic properties of each pseudo-component. The model parameters are fitted by experimental data for the mixture of tank oil with n-pentane and n-heptane. Optimized values of parameters are shown in Table 11. Table 12 gives the comparison of experimental and predicted amounts of asphaltene precipitation for various solvents at various dilution ratios. The agreement between experimental and predicted amounts of asphaltene precipitation is not very good.

Extended Ploydispersed Thermodynamic Molecular Model

As discussed previously, this model is the combination of the polydispersed molecular thermodynamic model and the wax model. Another model parameter η is introduced to account for the deposition from other components than plus fraction. Based on the fact that lower molecular weight compounds appear in the solids, we consider that four pseudo-components, FC22 through FC48, can form deposits in addition to the plus fraction from the Rangely oil.

This model is used on the experimental data of Rangely oil with n-pentane. Table 13 shows the model parameters and the comparison of experimental and predicted amounts of asphaltene precipitation. The new extended model gives better match between the experimental and predicted amounts of asphaltene precipitation than polydispersed thermodynamic molecular model.

Summary

Asphaltene precipitation models were first reviewed. Homogeneous thermodynamic model is based on the Flory-Huggins polymer theory to predict the amount of asphaltene precipitation due to the injection of solvents. The asphaltenes are considered as mono-dispersed polymeric molecules dissolved in the crude oil in this model. The crude oil is treated as a mixture of two liquid phases. The first phase is pure asphaltene liquid phase which acts as a solute and the second phase is the remaining components of the crude oil which acts as a solvent. The model predictions show good agreement with the experimental data after regression of asphaltene properties such as molar volume and solubility parameter. One limitation of this model is that parameters fitted with experimental data at low pressure are not useful in predicting asphaltene precipitation at

higher pressure since the molar properties of liquid phase will change along with the pressure.

Polydispersed thermodynamic molecular model is based on Scott-Magat theory. Asphaltenes are considered as heterogeneous molecules with a normal distribution of molecule weight. In predicting precipitation from various solvents, the model performance was better than the homogeneous model. This model allows for the effect of solvent weight through the use of interaction parameter between asphaltene and asphaltene-free phase. It also allows for incorporation of the effects of temperature and pressure on asphaltene properties such as molar volumes and solubility parameters.

Extended polydispersed thermodynamic molecular model was developed by combining the polydispersed thermodynamic molecular model and the wax model. Experimental evidence suggested that lower molecular weight compounds (with molecular weights as low as 300) were present in the deposits. Hence a provision was made for the incorporation of these compounds. It is a more realistic representation of asphaltene deposition from crude oils. This model gives a better match than the polydispersed thermodynamic molecular model between the experimental and predicted amount of asphaltene precipitation from the mixture of Rangely oil with n-Pentane.

Nomenclature

a Peng Robinson EOS Constant

a' Model Parameter

a_L Peng Robinson EOS Constant

A Peng Robinson EOS Constant

b Peng Robinson EOS Constant

b' Model Parameter

b_L Peng Robinson EOS Constant

B Peng Robinson EOS Constant

C_p Molar Heat Capacity

f Parameter Defined in Polydispersed Model

f_i Fugacity

F Objective Function

$F(M_A)$ Normal Distribution Function

G Gibbs Free Energy

H Enthalpy

K_i Solid-Liquid Equilibrium Constant in Wax Model

K_{AB} Interaction Parameter between Asphaltene and Asphaltene-free Liquid

K_{Ai} Solid-Liquid Equilibrium Constant in Polydispersed Model

M Molecular Weight

N Number of Components

NF Number of Asphaltene Free Components

R Gas Constant

P Pressure

P_c Critical Pressure

S Entropy

SG Specific Gravity

T Temperature

T_c Critical Temperature

T_r Reduced Temperature

U Internal Energy

V Molar Volume

W Weight Percent

x Molar Fraction

X Molar Fraction

Z Compressibility Factor

Greek Letters

α Peng Robinson EOS Constant

β Model Parameter

θ Model Parameter

δ Solubility Parameter

ϕ Volume Fraction

μ Chemical Potential

ρ Density

σ Standard Deviation of Normal Distribution Function

σ_{ij} Binary Interaction Parameters in EOS

ω Accentric Factor

ζ Variable Defined in Normal Distribution Function

γ Activity Coefficient

Subscripts and Superscripts

A Asphaltene

AD Deposited Asphaltene

Ai ith Fraction of Asphaltene

AT Total Asphaltene

B Asphaltene-free Liquid

F Fusion

i ith Fraction or Component

j jth Fraction or Component

L Liquid

Lmix Solvent-Oil Mixture

m Maximum

o Reference State

S Solid

TO Tank Oil

V Vaporization

+ Plus Fraction

Table 3: Elemental analyses (Weight Percent) of various asphaltenes (Speight, 1991)

Source	C	H	N	O	S
Canada	79.0	8.0	1.0	3.9	8.1
Canada	87.9	7.6	2.2	1.8	0.5
Iran	83.7	7.8	1.7	1.0	5.8
Kuwait	82.4	7.8	0.9	1.5	7.4
Venezuela	84.0	7.9	2.0	1.6	4.5
Mexico	81.4	8.0	0.6	1.7	8.3

Table 4: Hirschberg tank oil composition

Composition	(mol%)
C1	0.10
C2	0.48
C3	2.05
iC4	0.88
nC4	3.16
iC5	1.93
nC5	2.58
C6	4.32
C7+	84.50
Average MW of tank oil	221.50
Specific gravity of tank oil	0.873
Average density of asphaltene, g/cm^3	1.2

Table 5: Optimized values of parameters for different solvents (Hirscberg oil)

Solvent	δ_A $(Psia)^{0.5}$	V_A $(ft^3/lbmole)$
nC5	383.6	0.22
nC7	386.3	0.18
C10	303.2	0.54

Table 6: Experimental data compared to prediction for amount of asphaltene precipitation from Hirschberg tank oil

Solvent	Dilution Ratio (cm^3 solvent/g tank oil)	Experimental wt %	Calculated wt %
NC5	10.0	3.61	3.7258
	20.0	3.79	3.7522
	50.0	3.87	3.7694
NC7	5.0	1.53	1.7213
	10.0	1.82	1.7495
	20.0	1.89	1.7659
	50.0	1.87	1.7760
C10	5.0	1.34	1.3546
	10.0	1.45	1.4438
	20.0	1.50	1.4958

Table 7: Optimized values of parameters for Hirschberg tank oil

Solvent	β	σ	a'	b'
nC5	0.00665	194.0	0.155	-0.0010
C6	0.00495	142.0	0.1875	-0.001225
C7	0.00325	90.0	0.22	-0.00145
C10	0.0026	65.0	0.26	-0.00135

Table 8: Experimental data compared to prediction for amount of asphaltenes from the Rangely crude oil

Solvent	Dilution Ratio (cm^3 solvent/g tank oil)	Experimental, wt %	Calculated, wt %
nC5	0.0	---------	0.0045
	1.0	---------	0.0201
	2.0	---------	3.0858
	3.0	---------	3.4584
	4.0	---------	3.5541
	5.0	---------	3.6037
	10.0	3.61	3.6125
	20.0	3.79	3.8246
	50.0	3.87	3.8530
C6	0.0	---------	0.0036
	1.0	---------	0.0102
	2.0	---------	2.1200
	3.0	---------	2.5901
	4.0	---------	2.6907
	5.0	---------	2.8293
	10.0	---------	2.8334
	20.0	---------	2.8367
	50.0	---------	2.8427
C7	0.0	---------	0.0025
	1.0	---------	0.0010
	2.0	---------	0.0277
	3.0	---------	0.4989
	4.0	---------	1.3118
	5.0	1.53	1.5286
	10.0	1.82	1.8571
	20.0	1.89	1.8604
	50.0	1.87	1.8628
C10	0.0	---------	0.0021
	1.0	---------	0.0027
	2.0	---------	0.2055
	3.0	---------	1.1034
	4.0	---------	1.2772
	5.0	1.34	1.3447
	10.0	1.45	1.4862
	20.0	1.50	1.4875
	50.0	---------	1.4890

------- No data

Table 9: Composition of the Rangely crude oil obtained by simulated distillation

Component	Weight %	Component	Weight %
C5	2.791435	C34	1.246557
C6	2.797687	C35	1.241887
C7	1.718041	C36	1.085021
C8	2.700792	C37	0.920742
C9	4.148689	C38	0.989896
C10	3.762076	C39	0.869194
C11	4.495995	C40	0.765496
C12	3.691702	C41	0.696806
C13	3.895433	C42	0.681447
C14	4.152392	C43	0.581452
C15	4.072598	C44	0.610525
C16	3.347929	C45	0.597152
C17	3.679020	C46	0.574754
C18	2.566236	C47	0.500537
C19	3.310149	C48	0.503767
C20	2.840317	C49	0.495502
C21	2.749553	C50	0.455431
C22	2.573762	C51	0.425555
C23	2.509332	C52	0.410303
C24	2.084314	C53	0.402739
C25	2.348433	C54	0.353844
C26	1.972203	C55	0.383281
C27	1.956050	C56	0.350282
C28	1.866888	C57	0.344287
C29	1.943955	C58	0.302389
C30	1.603736	C59	0.335875
C31	1.519809	C60	0.277878
C32	1.462037	C60+	3.748586
C33	1.288221		

Table 10: Lumping the components of Rangely crude oil, obtained by simulated distillation into appropriate pseudocomponents

Pseudo-Component	Mol %	MW	Pc, atm	Tc, K	ω
FC6	18.2890	81.369	32.6097	496.984	0.26963
FC9	23.0875	124.147	26.4059	604.142	0.40552
FC13	19.7670	174.360	20.5644	681.250	0.55902
FC17	13.9581	238.085	16.3045	749.600	0.72765
FC22	9.5662	303.228	13.1965	806.019	0.88804
FC29	7.5221	400.210	10.8626	862.012	1.03476
FC38	5.6119	524.146	9.4314	912.732	1.14466
FC48	2.1928	666.512	8.2688	964.174	1.25311

δ_{ij}	FC6	FC9	FC13	FC17	FC22	FC29	FC38	FC48
FC6	0.00000							
FC9	0.00237	0.00000						
FC13	0.00817	0.00176	0.00000					
FC17	0.01595	0.00611	0.00133	0.00000				
FC22	0.02411	0.01156	0.00435	0.00088	0.00000			
FC29	0.03105	0.01659	0.00765	0.00262	0.00047	0.00000		
FC38	0.03798	0.02185	0.01138	0.00498	0.00168	0.00038	0.00000	
FC48	0.04465	0.02708	0.01529	0.00769	0.00339	0.00135	0.00030	0.00000

Table 11: Optimized parameters in the polydispersed thermodynamic model for the precipitation of asphaltenes from Rangely crude oil.

Solvent	β	σ	a'	b'
nC5	0.155	102.5	0.40	-0.0040
nC7	0.1040	210.0	0.34	-0.00245

Table 12: Experimental data and model predictions for amount of asphaltenes precipitated using various solvents; polydispersed thermodynamic model

Solvent	Dilution Ratio (ml solvent/ml tank oil)	Experimental, wt %	Calculated, wt %
nC5	0.0	---------	0.0033
	1.0	---------	0.0033
	2.0	---------	0.0035
	3.0	---------	0.0038
	4.0	---------	0.0554
	5.0	1.91	1.9027
	10.0	2.18	2.4782
	20.0	2.69	2.4784
	40.0	2.65	2.4781
	50.0	---------	2.4781
nC7	0.0	---------	0.0021
	1.0	---------	0.0021
	2.0	---------	0.0028
	3.0	---------	0.6577
	4.0	---------	1.4402
	5.0	1.71	1.6717
	10.0	1.95	1.6662
	20.0	1.42	1.6650
	40.0	1.78	1.6652
	50.0	---------	1.6659

---------Data not available

Table 13: Experimental data and model predictions for amount of asphaltenes precipitated using various solvents; extended polydispersed thermodynamic model

Solvent	Dilution Ratio (ml solvent/ml tank oil)	Experimental, wt %	Calculated, wt %
nC5	0.0	---------	0.0007
	1.0	---------	0.0007
	2.0	---------	0.0009
	3.0	---------	0.0409
	4.0	---------	0.0448
	5.0	1.91	1.9084
	10.0	2.18	2.2850
	20.0	2.69	2.5850
	40.0	2.65	2.6185
	50.0	---------	2.6278
Model Parameters:	η=0.01	β=0.1465	σ =114.0
	a'=0.39	b'=-0.0041	

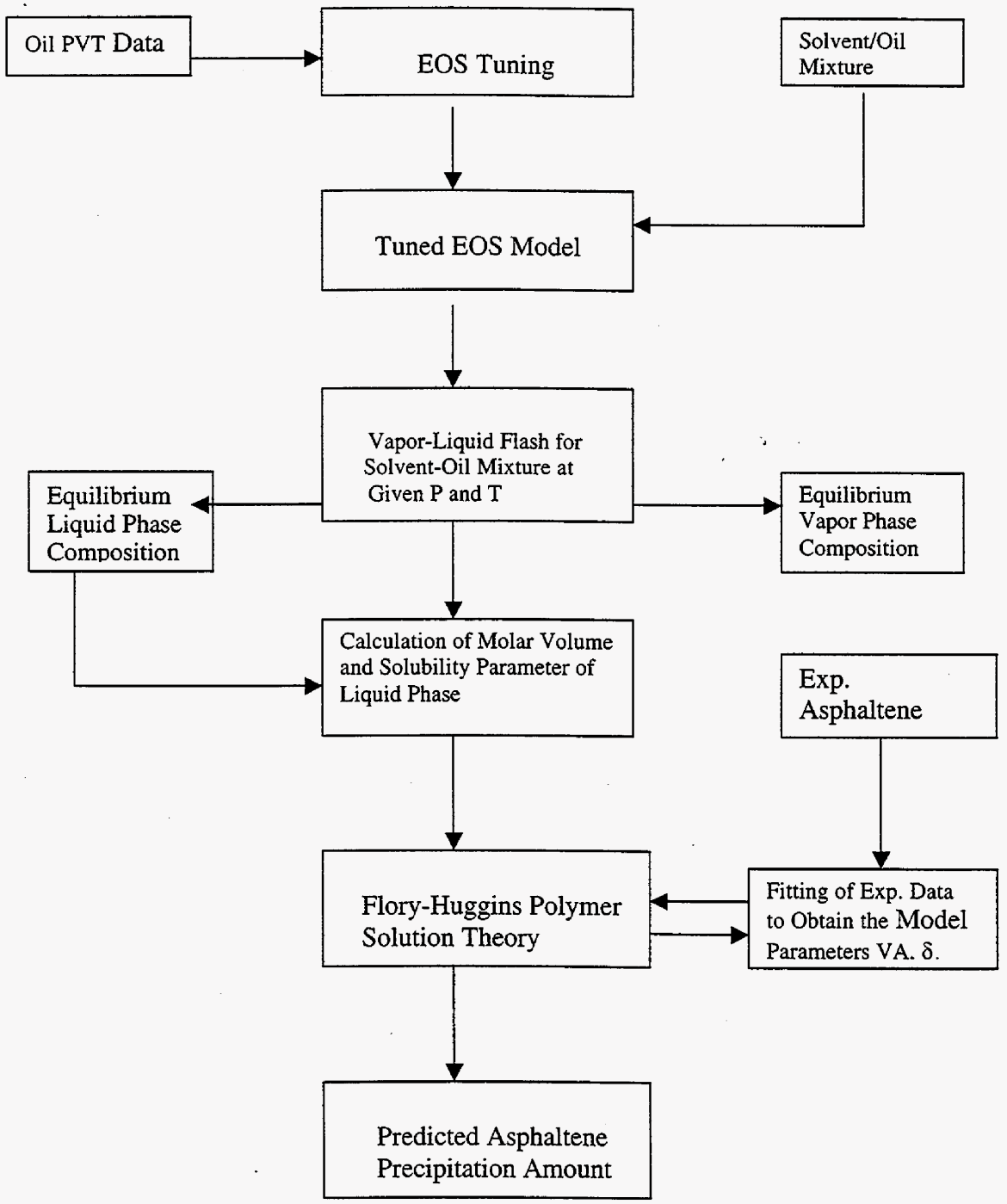

Figure 14: Flow Diagram of homogeneous molecular thermodynamic model

Figure 2 Flow Diagram of Polydispersed Molecular Thermodynamic Model

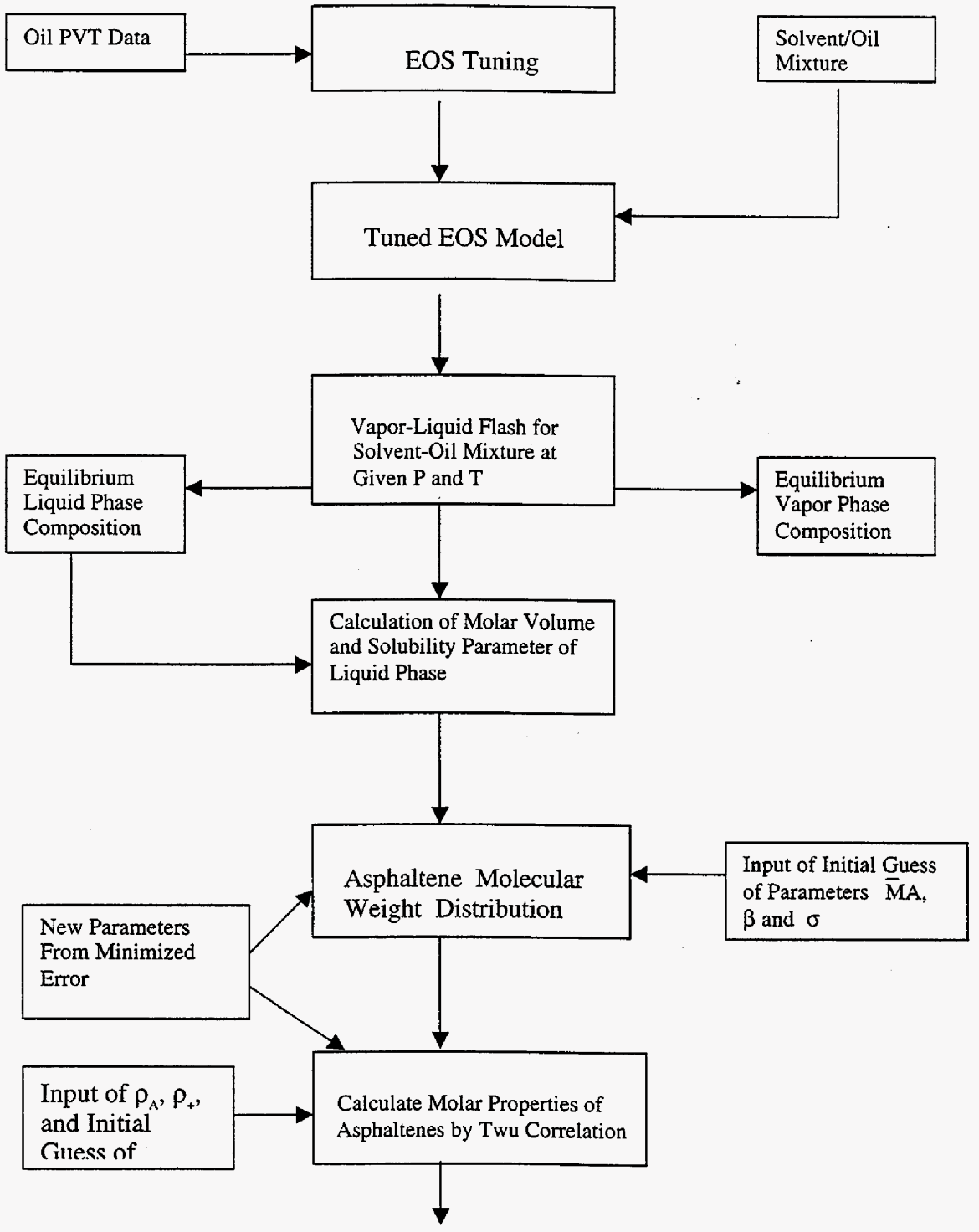

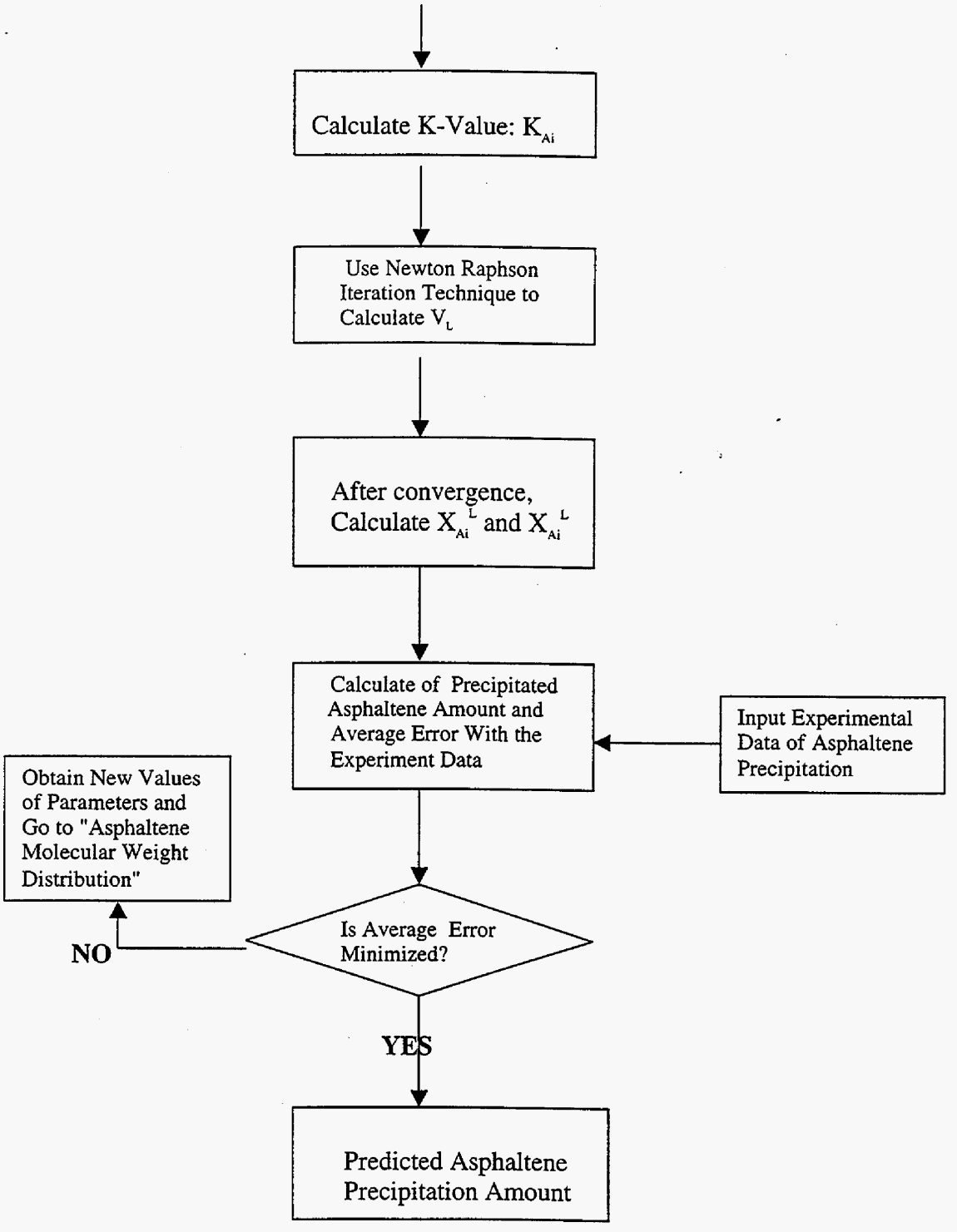

Figure 15: Flow diagram for performing thermodynamic calculations using the polydispersed thermodynamic model

Pure-component thermodynamic experiments

A liquid mixture containing varying amounts of toluene and phenanthrene were mixed with a mixture containing hexane and small amounts of phenanthrene to simulate the precipitation of asphaltenes. The solid-liquid equilibrium was completely mapped for this system and is shown in Figure 16.

Use of a solid-liquid equilibrium model was investigated to describe the results.

When the solvent does not enter the solid phase, the fugacity of the solid solute remains that of pure solid, so the condition of equality of partial fugacities at equilibrium becomes (Walas, 1985)

$$\hat{f}_{2(soloid)} = f_{2(solid)} = \gamma_2 x_2 f_{2(subcooled\_liquid)}$$

Which means that

$$x_2 = \frac{f_{2s}}{\gamma_2 f_{2(scl)}},$$

where x_2 is the mol fraction of the solute in the solution and $f_{2(scl)}$ represents the fugacity of the pure solid solute in a subcooled liquid state below its melting point.

The general solubility equation for x_2 is given by:

$$x_2 = \frac{1}{\gamma_2}\exp\left[\frac{\Delta H_{tp}}{R}\left(\frac{1}{T_{tp}}-\frac{1}{T}\right)-\frac{\Delta Cp}{R}\left(\ln\frac{T_{tp}}{T}-\frac{T_{tp}}{T}+1\right)-\frac{\Delta V}{RT}\left(P-P_{tp}\right)\right]$$

In the above equation, the subscript *tp* designates the triple point.

This form of the equation applies when the heat capacity difference is relatively insensitive to temperature.

When the pressure and heat capacity differences are neglected,

$$x_2 = \frac{1}{\gamma_2}\exp\left[\frac{\Delta H_{tp}}{R}\left(\frac{1}{T_{tp}}-\frac{1}{T}\right)\right] = \frac{1}{\gamma_2}\exp\left[\frac{\Delta S_{tp}}{R}\left(1-\frac{T_{tp}}{T}\right)\right]$$

where $\Delta S_{tp} = \Delta H_{tp} / T_{tp}$ is the entropy of fusion at the triple point.

Since triple-point temperatures usually are very close to melting points the solubility equation is often written in terms of properties at this better known property.

$$x_2 = \frac{1}{\gamma_2}\exp\left[\frac{\Delta H_m}{R}\left(\frac{1}{T_m}-\frac{1}{T}\right)\right] = \frac{1}{\gamma_2}\exp\left[\frac{\Delta S_m}{R}\left(1-\frac{T_m}{T}\right)\right]$$

where the subscript m identifies conditions at the atmospheric melting point.

The above equation is used with of the Scatchard-Hildebrand equation for the activity coefficient of the solute which requires only properties of pure components.

$$\gamma_2 = \exp\left[\frac{\Delta S_m}{R}\left(1-\frac{T_m}{T}\right)-\frac{V_2\phi_1^2(\delta_1-\delta_2)}{RT}\right],$$

where,

$$\phi_1 = \frac{V_1 x_1}{V_1 x_1 + V_2 x_2}$$

The equations below are used for the calculation of the phenanthrene solubility in toluene and hexane mixture.

$$x_2 = \exp\left\{-\left[\frac{\Delta H_m}{R}\left(\frac{1}{T}-\frac{1}{T_m}\right)+\frac{V_2}{RT}\left[\frac{\delta_1-\delta_2}{1+\frac{V_2 x_2}{V_1(1-x_2)}}\right]^2\right]\right\}$$

Mean solubility parameter is given by:

$$\bar{\delta} = \frac{\sum x_i V_i \delta_i}{\sum x_i V_i}$$

$$x_2 = \exp\left\{-\left[\frac{\Delta H_m}{R}\left(\frac{1}{T}-\frac{1}{T_m}\right)+\frac{V_2}{RT}\left[\frac{\delta_1-\bar{\delta}}{1+\frac{V_2 x_2}{V_1(1-x_2)}}\right]^2\right]\right\}$$

There were significant differences in literature values of various parameters required. Basic pure component properties are shown in Table 14. Variations in properties of phenanthrene important in determining solid-liquid equilibria are shown in Table 15.

Solubilities calculated using various combinations are compared to experimental results in Figure 16. The comparison shows that a melting point of 373.15 K, a solubility parameter of 9.922 and a heat of fusion of 4300 cal/mol are the phenanthrene properties that provide a good match between the experimental data and the solubility model predictions.

Table 14: Basic pure component properties in the solubility model

	Molecular weight (g / mol)	δ, solubility parameter (cal / cm^3)$^{0.5}$	V, molar volume (cm^3 /mol)
Phenanthrene	178.23	9.922	158
Hexane	86.18	7.27	131.51
Toluene	92.14	8.93	106.84

Table 15: Comparison of physical properties of phenanthrene appearing in different references

Reference	Heat of fusion (cal/mol)	Melting temperature (°C)	Solubility parameter (cal/cm^3)$^{0.5}$
Prausnitz, et al.		100	9.922
Perry's Handbook	4455		
Gordon and Scott	4300	96.3	9.8*
Barton - CRC			9.775**
David Lide - CRC	3921	99.24	

*estimated

** Hilderbrand solubility parameter

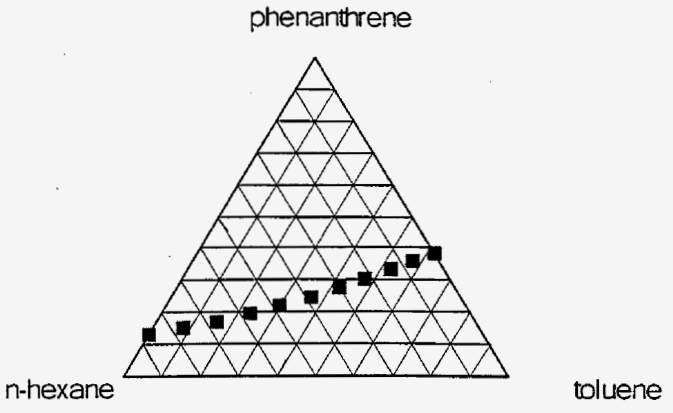

Figure 16: Ternary diagram for phenanthrene, hexane and toluene (weight percents)

Kinetic Measurements and Modeling

Experiments were performed in which 10 ml of Rangely oil was placed in an insulated vessel. In the vessel is a magnetic stirrer and a thermocouple to record the temperature. The temperature is recorded as a solvent (either pentane, hexane or heptane) was added at a constant flow rate of either 1 ml/min or 2.5 ml/min. An example of the experimental results is given in Figure 17, where pentane at a flow rate of 1 ml/min is mixed with oil. It is seen that the temperature initially rises and then decreases, then finally increases. This curve appears to be the result of the superposition of two curves: 1) the initial quick rise and 2) a slowly increasing temperature profile. The initial quick rise is over by 600 sec corresponding to the point where the mole fraction solvent has reached 0.5. In this sample, some asphaltenes were precipitated by the pentane addition. Analysis of this type of curve was performed by considering the energy of mixing, heat of mixing two liquids and heat of precipitation of the asphaltene fraction.

Consider mixing of oil with a solvent when asphaltene precipitation does not takes place. When the solvent feed temperature and the initial temperature of oil in the vessel are the same, T_0, then the overall energy balance is given by:

$$(V_o + Qt)\frac{C_v}{v}\frac{d(T-T_o)}{dt} = E_{mix} + (V_o + Qt)\frac{\partial(\nabla H_m)}{d\Phi_1}\frac{\partial\Phi_1}{\partial t}$$

As written, this equation assumes that the heat capacity, C_v, and the molar volume, v, are constant, however, this can be changed if necessary. This assumption is reasonable, if the heat capacity and molar volume of the solvent and oil are similar or more precisely if their ratio does not vary as the solvent mole fraction is increased from zero to 0.5 and beyond. Other quantities in the equation are given by:

Mixing Energy per unit time = E_{mix}

Heat of mixing per unit volume, $\nabla H_m = \Phi_1(1-\Phi_1)(\delta_1 - \delta_o)^2$.

where Φ_1 is the volume fraction solvent and δ is the solubility parameter for the solvent, subscript 1, and for the oil, subscript o. At any time the volume fraction of solvent is $\phi_1 = Qt/(V_o+Qt)$. The volume fraction and the mole fraction (X) are related by:

$$\phi_1 = \frac{\nu_1 X_1}{\nu_1 X_1 + \nu_o X_o}$$

where ν is the molar volume with subscript 1 corresponding to solvent and subscript o to oil. When oil is modeled as a true multicomponent mixture, a method to evaluate mixture molar volume and equivalent solubility parameter will have to be developed.

In the above, Scatchard and Hildebrand regular solution theory is used for the formulation of the heat of mixing. Upon integration the temperature difference, $\Delta T=T-T_o$, is given by:

$$\Delta T(t) = T(t) - T_o = \frac{\nu}{C_v}\left[\frac{\ln(1+\frac{Q\,t}{V_o})}{Q} V_o E_{mix}\right] + \frac{\nu}{C_v}\left[\frac{Qt}{V_o+Qt}(1-\frac{Qt}{V_o+Qt})(\delta_1-\delta_o)^2\right]$$

In this equation, there are two terms; the first corresponding to mixing which slowly grows with time and the second which first increases then decreases due to the effects of the $\Phi_1(1-\Phi_1)$ term as the volume fraction of solvent increases. Figure 18 shows the separate effects of various values of E_{mix} and $(\delta_1-\delta_o)$ on $\Delta T(t)$. Increasing the value of o increases the height of the peak observed at 10 min. At 10 minutes, the mole fraction of solvent is 0.5 corresponding to a maximum in the $\Phi_1(1-\Phi_1)$ term. Since the precipitation takes place when the mole fraction of the solvent is changing the most, i.e. in the first 10 minutes, we can use this equation for the long time effects on the temperature and by curve fitting determine the unknowns, E_{mix} and $(\delta_1-\delta_o)^2$.

Since the maximum in the experimental data occurs at a time of approximately 100 seconds, and not 10 minutes, we can be assured that the initial quick rise is not due to solvent mixing but to precipitation of asphaltenes. Thus, we can use the best fit of the temperature difference equation for the long time data, t>30 min, and extrapolating back to shorter times we can clearly identify the differences that must be due to precipitation. The difference between the fit and the data at short times corresponds to the enthalpy due to precipitation of asphaltenes. Figure 19 is a plot of the temperature effect of this

precipitation. The point of deviation of the experimental data from the fit curve in Figure 4, indicates the mole fraction at which asphaltene is supersaturated in the system. In this case, it is essentially immediately. Precipitation appears to stop after 10 minutes. Calculations are being continued at the present time to determine the enthalpy of precipitation (mass of asphaltenes precipitated and molecular weight of asphaltenes are necessary for this exercise).

Regular solution theory can also be used to identify the asphaltene solubility, $X_{a,eq}$.

$$-RT\ln X_{a,eq} = \Delta H_{F,a} + v_a \phi_s^2 (\delta_s - \delta_a)^2$$

$$= \Delta H_{F,a} + v_a \left(\frac{v_1 X_1 + v_o X_o}{v_1 X_1 + v_o X_o + v_a X_a}\right)^2 ((\delta_1 X_1 + \delta_o X_o + \delta_a X_a) - \delta_a)^2$$

where R is the gas constant, T is the temperature, $\Delta H_{F,a}$ is the heat of fusion of asphaltene at a reference temperature ,T_R, v_a is the molar volume of asphaltene, δ_a is the solubility parameter of asphaltene, ϕ_s is the volume fraction of the solvent system (oil plus solvent at any time) and δ_s is the solubility of the solvent system. The heat of fusion for asphaltene can be measured by differential scanning calorimetry of the precipitated solid. As the volume fraction of solvent (subscript, 1) is increased the volume fraction of the system approaches 1.0 and the value of the solubility parameter decreases to a value near that of the solvent. The result of both of these effects is to decrease the solubility of asphaltene as solvent is added as shown in Figure 20. Also shown is an assumed concentration of asphaltene. Initially the solution is undersaturated. At the intersection of the two curves in Figure 4, the solution is saturated. At higher mole fractions of solvent, X_1, the solution is supersaturated. The supersaturation ratio, Xa/Xeq, is the driving force for precipitation.

Titration Kinetics

Kinetics of precipitation of asphaltenes with liquid solvents were measured. The data used in the analysis is shown in Figure 21. A simple kinetic model was used to fit the data.

$$1-\frac{W}{W_{max}}=\exp(-kt)$$

W: Weight of the precipitate as a function of time (as a percentage of the original oil)

W_{max}: Maximum weight percent precipitated

k: rate constant

t: time(hours)

k values for a number of solvents are listed in Table 16. The rate constant decreases as the solvent carbon number increases.

Table 16: Rates of asphaltene precipitation with liquid solvents

Solvent	**K-value (1/hour)**
Pentane	1.90
Hexane	1.35
Heptane	1.16

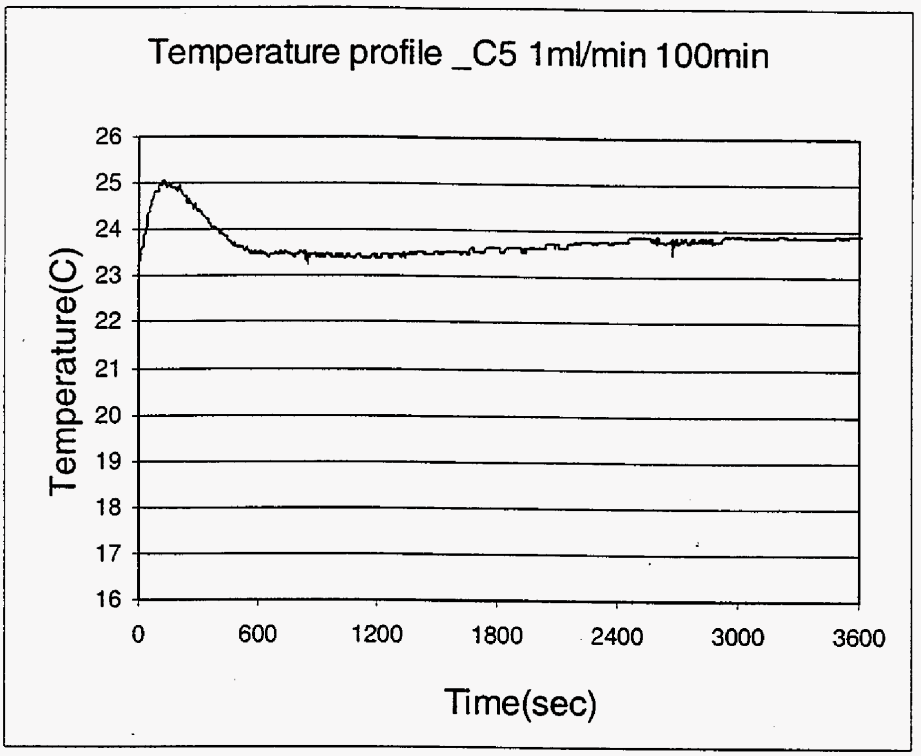

Figure 17: Temperature observation due to mixing of pentane at a flow rate of 1 ml/min into 10 ml of Rangely crude

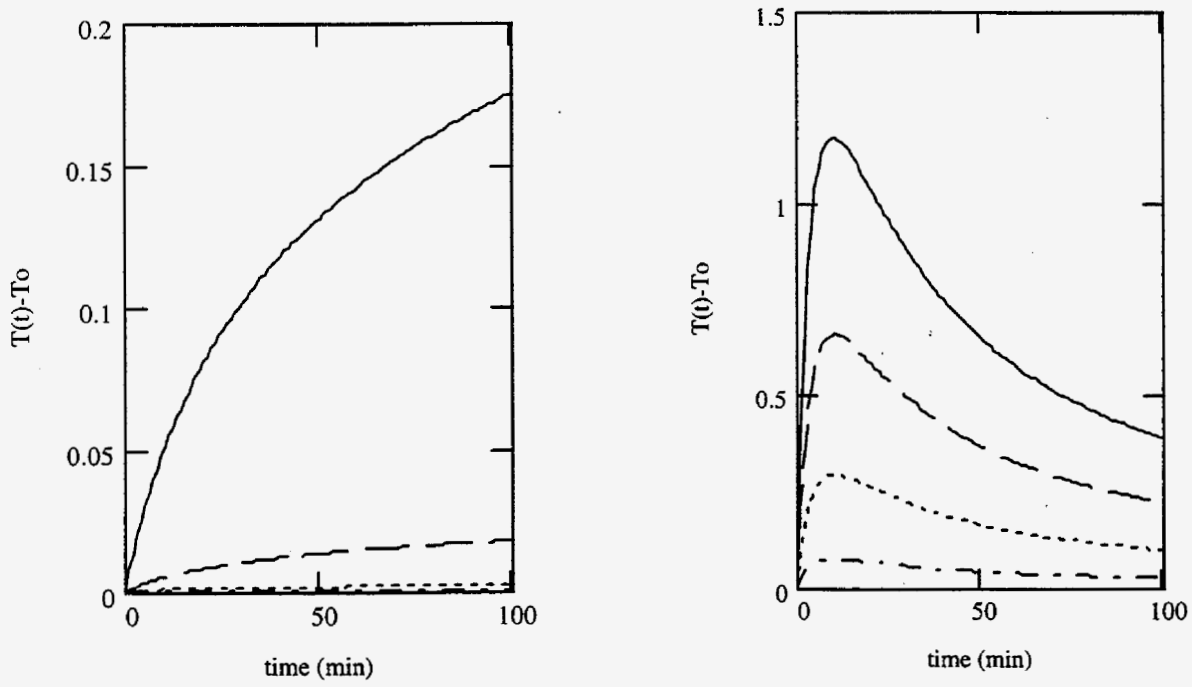

Figure 18: Effect of Emix and (d1 -do) on DT(t) (°C). (a) Effect of various values of (d1 -do) on DT(t) assuming Emix is zero, for curves from bottom to top (d1 -do) = 7.3, 7.5, 7.7, 7.9, (b) Effect of various values of Emix on DT(t) assuming (d1 -do) is zer

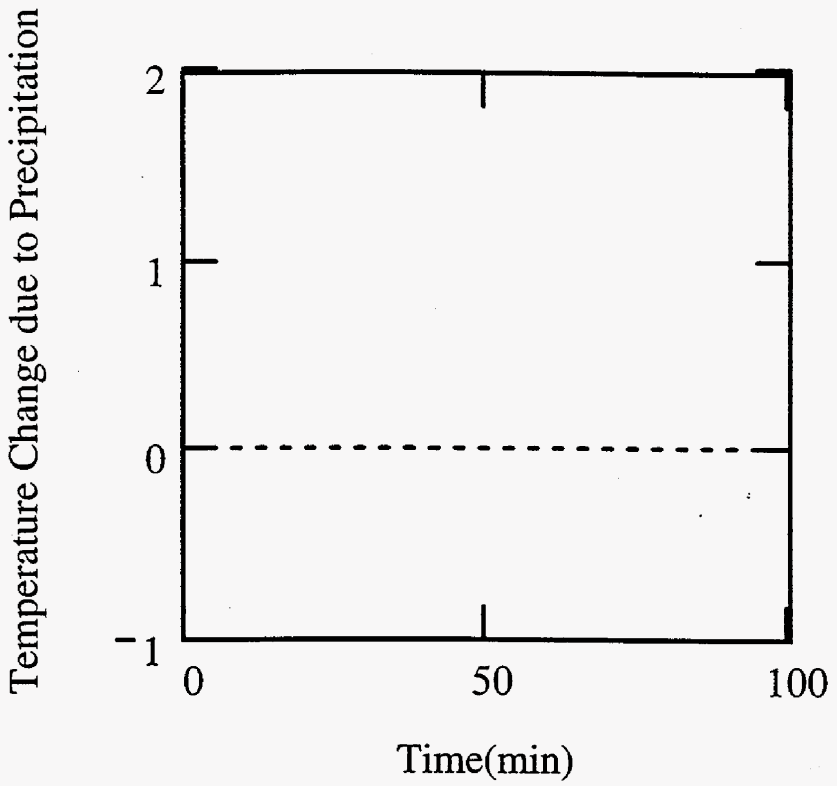

Figure 19: Difference in the experimental and curve fit of long time data identifying the temperature change due to the enthalpy of asphaltene precipitation

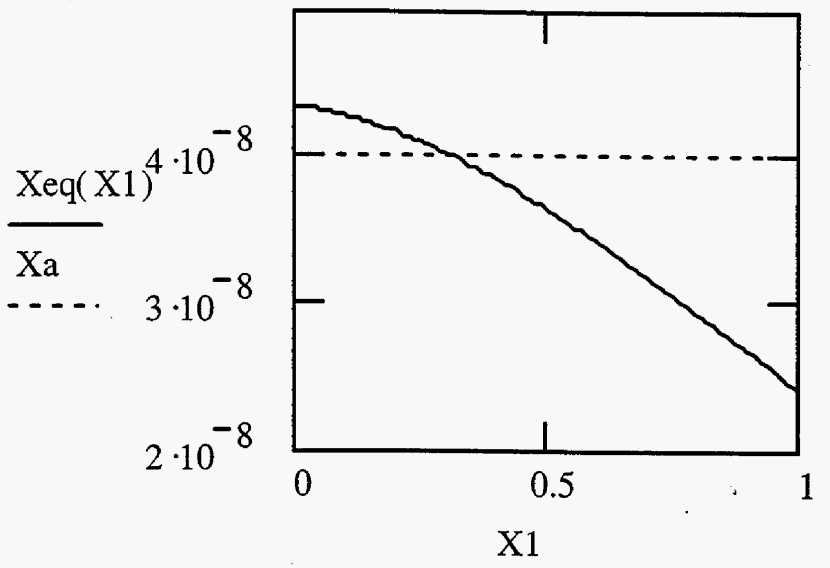

Figure 20: Solubility of asphaltene, Xeq, (solid line) and asphaltene, Xa, (dashed line), in solution assumed to be 4x10-8 as the solvent mole fraction, X1 is increased. Depending upon the amount of asphaltene in the oil, the point at which the solution is satur

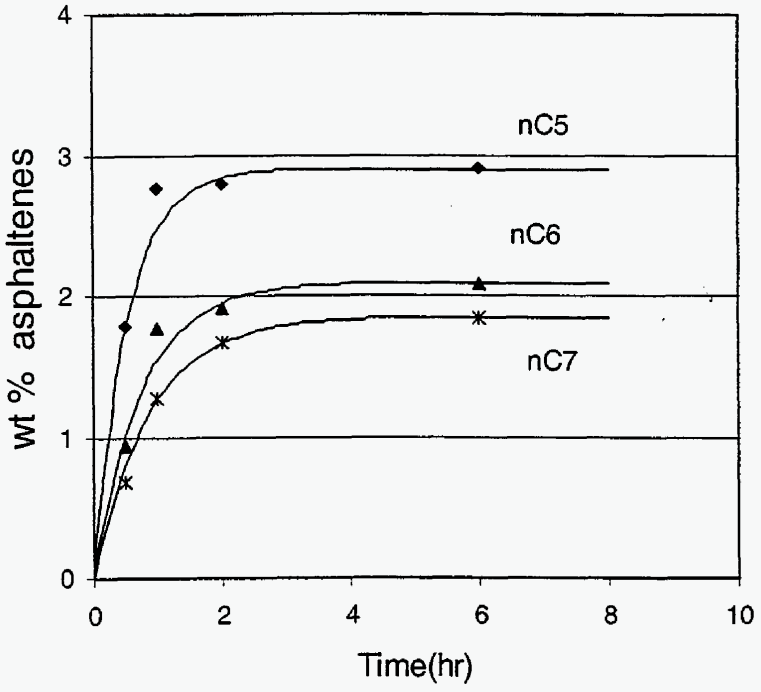

Figure 21: Precipitation of asphaltenes as a function of time

Core Floods

Previous core floods confirmed the compositional changes taking place in a carbon dioxide flood. The core flood performed during this period was essentially to see if these compositional changes were causing added precipitation in the core. One additional objective was to examine the behavior of fluids exiting from the core when subjected to a "wellbore" flash.

The high-pressure, core flooding experimental setup described earlier was used with some modifications. The core outlet was connected to two visual (PVT) cells. These cells were filled with carbonated brine at system conditions prior to the carbon dioxide core flood.

The sequence of operations and results were as follows. The core was mounted in a triaxial core holder and was pressurized to about 3000 psia. The pore volume of the core was recorded using volume expansion measurements. Approximately 12 different pressure cycles were used and the pore volume was averaged. The pore volume was 39 cc. The core was six inches long and was 1.5 inches in diameter for a total volume of 174 cc. The porosity of the rock was thus 22 %. The core was saturated with CO_2 at about 100 psia and was flooded with brine. After brine breakthrough, the fluids were pressurized to 2000 psia; the brine flood continued for about four PV.

The Rangely crude was introduced into the core. A total of about 4 PV of oil was sent through the core. The oil exited the core through 2 filters, a 2 micron filter and a 0.5 micron filter. This was basically to obtain a baseline for solids movement and deposition on filters without any compositional changes. The solids collected amounted to 0.1562 g or about 0.13% of the oil flowed through the filters. The core was sealed, the filters were returned online.

CO_2 was flooded through the core at 2000 psia. The oil exiting the core was filtered and collected in two high-pressure PVT cells. The PVT cells originally contained carbonated brine and thus simulated production wells. The amount of solids collected were 0.55 g for a total of 26 g of oil exiting the core. If the baseline solid value is subtracted (0.13%), this amounts to 2% solids from the oil exiting the core. The first contact precipitation amounts were all less than 1% (with the exception of one experiment, which is being repeated). Thus, the multiple contact mixture generated in the core has a tendency to

precipitate twice the amount of solids as single-contact mixtures at any CO_2 concentration.

The high-pressure, oil-CO_2 mixtures collected in the PVT cells were flashed and sampled to assess the tendency of these mixtures to form solids. As a gas bubbles form and leave the flash chamber, they appeared to deposit some solid material on fittings and tubing. This was estimated to be only about 0.06% of the oil in the chamber. The oil in both the chambers was filtered and the solids collected and weighed. The total amount of solids collected amounted to 0.11% which, given the margin of error in the measurements was close to the baseline solids amount in the oil. Thus, almost all of the solids precipitated in the multiple contact mixture were trapped at the core outlet.

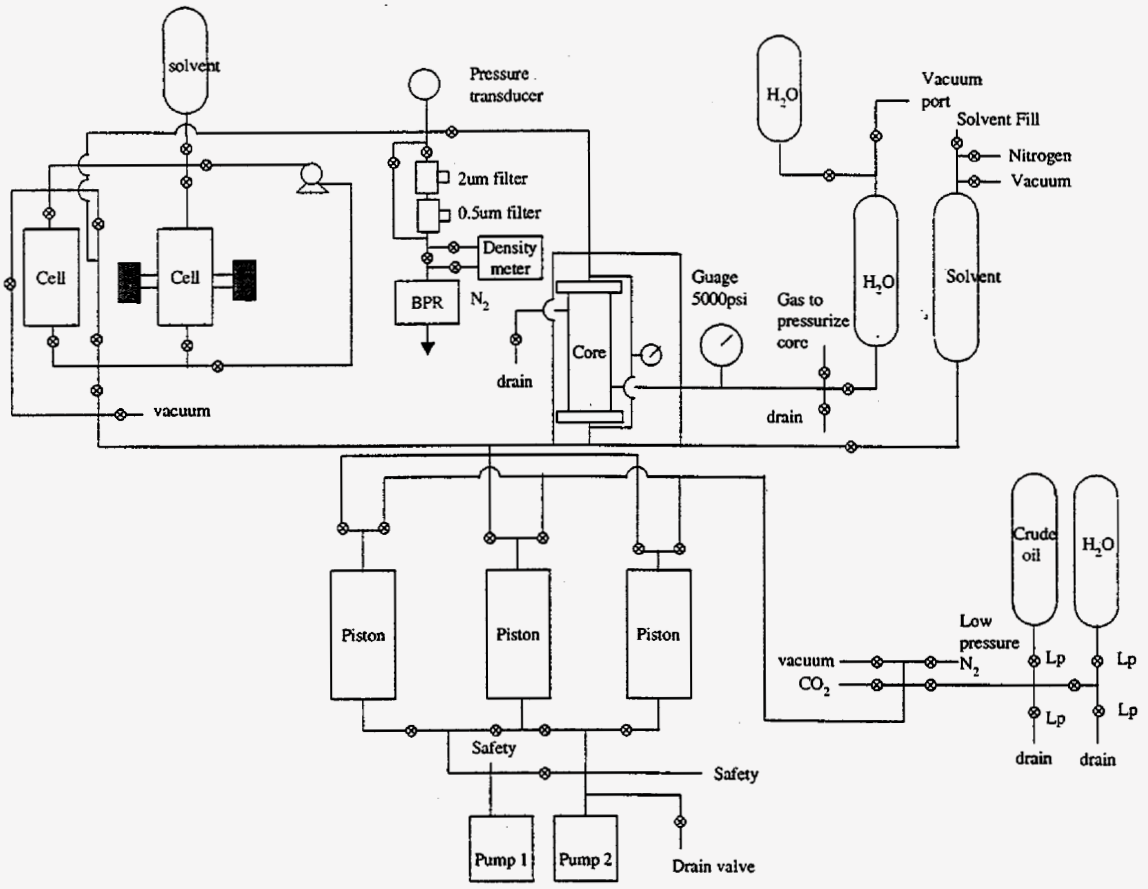

Figure 22: Experimental configuration used for the wellbore flash experiments

Compositional Simulations

An efficient, multidimensional equation-of-state (EOS) compositional simulator, GEM from Computer Modeling Group, Calgary was used to simulate one-dimensional carbon dioxide floods. The simulations were streamlined by first simulating a pure-component system. Pure component system consisted of CO_2, n-butane and n-decane, for which the phase behavior is well known. A more realistic oil composition (shown in Table 17) was simulated at three different pressures; 2100 psia , where first-contact miscible displacement is expected to occur, 1500 psia, where multiple-contact miscible displacement is expected and 1000 psia, where immiscible displacement occurs. Recovery plots at the three different pressures are shown in Figure 23. Progressively, the oil recovery decreases as we go from FCM to MCM to immiscible. More significant is the compositional change that accompanies each displacement. The implication of this compositional change on asphaltene precipitation is currently being investigated.

Table 17: Initial composition of the crude simulated in one-dimensional compositional simulations

Component	Mole Fraction
CO_2	0
n-C_4	0.1
Pseudo-component FC_{10}	0.3
Pseudo-component FC_{16}	0.3
Pseudo-component FC_{30}	0.2
Pseudo-component FC_{45}	0.1

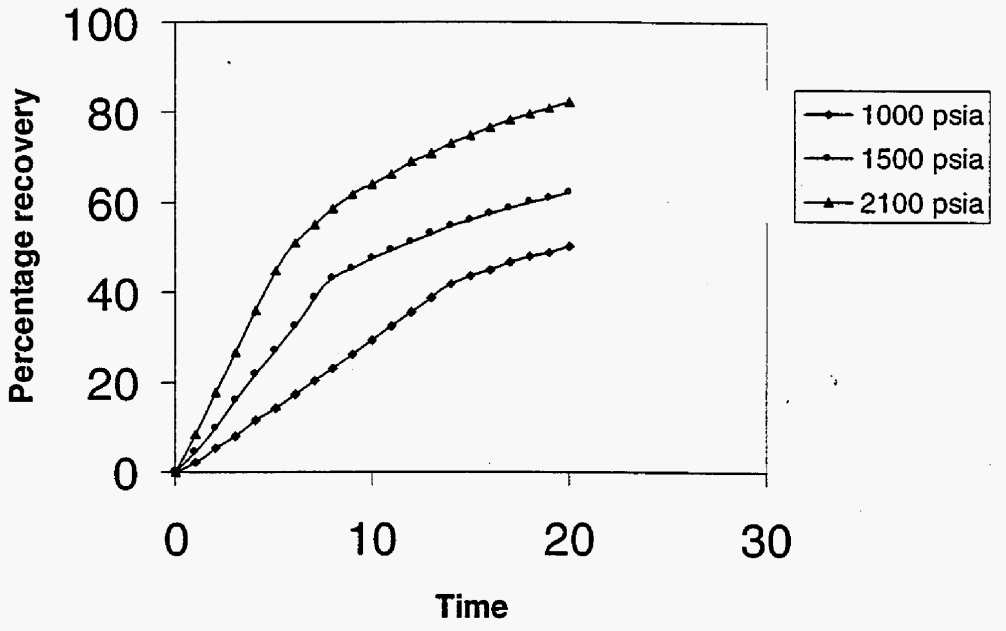

Figure 23: Recovery profiles (using compositional simulations) for first-contact miscible (2100 psia), multiple-contact miscible (1500 psia) and immiscible (1000 psia)

References

Barton, A. F. M., 1983, *"CRC Handbook of Solubility parameters and other Cohesion parameters"*, CRC Press.

Burke, N.E. et al., 1990, "Measurement and modeling of asphaltene precipitation", Journal of Petroleum Technology (Nov. 1990) 1440.

Ferworn, K.A., 1995, "Thermodynamic and Kinetic Modeling of Asphaltene Precipitation from Heavy Oils and Bitumens", *Ph.D. Thesis of University of Calgary,* 1995.

Gambill, G. A., 1957, "Determine Heat of Vaporization", Chem. Eng., 64(12), 1957, p.261.

Graue, D. J. and Zana, E.T., 1981, "Study of possible CO_2 flood in Rangely field", Journal of Petroleum Technology (Jul. 1981) 1312.

Hansen, J. H., et al., 1988, "A Thermodynamic Model for Predicting Wax Formation in Crude Oils", *AIChE Journal, 34(12),* 1988, p. 1937.

Hervey, J.R. and Iakovakis, A.C., 1991, "Performance review of miscible CO_2 tertiary project: Rangely Weber Sand Unit, Colorado", SPE Reservoir Engineering (May 1991) 163.

Hirschberg, A. et al., 1984, "Influence of temperature and pressure on asphaltene flocculation", SPEJ (Jun. 1984) 283.

Kawanaka, S. and Mansoori, G.A, 1991, "Organic Deposition from Reservoir Fluids: A Thermodynamic Predictive Technique", SPE Reservoir Engineering, 32(5), 1991, p. 185.

Kokal, S.L. and Sayegh, S.G., 1995, "Asphaltenes: the cholesterol of petroleum", paper SPE 29787 (1995) 169.

Gordon, L. J. and Scott, R.L., 1992, , J. Am. Chem. Soc.,74:4138.
Lide, D. R., 1992, *CRC Handbook of Chemistry and Physics* 73rd, CRC Press.

Leontaritis et al., 1989, "Asphaltene Deposition: A Comprehensive Description of Problem Manifestations and Modeling Approaches", *SPE 18892,* 1989.

Lira-Galeana C. and Firoozabadi, A., 1996, "Thermodynamic of Wax Precipitation in Petroleum Mixtures", *AIChE Journal, 42(1), 1996*, p. 239.

Long, R.B., 1981, "The Concept of Asphaltene", *Chemistry of Asphaltene, Advances in Chemistry series, 195*, 1981, p. 17.

Mansoori, G.A., 1988, "Asphaltene Deposition and Its Role in Petroleum Production and Processing", *The Arabian Journal for Science and Engineering, 13(1),* 1988, p. 17.

Mitchell, D.L. and Speight, J.G., 1973, "The Solubility of Asphaltenes in Hydrocarbon Solvent", *Fuel, 52,* 1973, p. 149.

Monger, T.G. and Fu, J.C., 1987, "The nature of CO_2-induced organic deposition", paper SPE 16713 (Sept. 1987) 147.

Monger, T.G. and Trujillo, D.E., 1991, "Organic deposition during CO_2 and rich-gas flooding", SPE Reservoir Engineering (Feb. 1991) 17.

Nghiem, L., 1993, "Efficient Modeling of Asphaltene Precipitation", *SPE 26642,* 1993.

Nghiem, L., 1996, "Modeling Effects on Asphaltene Precipitation", *Hydrocarbon Technology International, Sterling Publications International Limited, London,* 1996, p. 75.

Nighswander, J.A. et al., 1993, "Effect of Low molecular weight hydrocarbons on the onset concentration and bulk properties of asphaltene at in-situ temperature and pressure conditions", Paper 55E presented at the AIChE meeting (March 28, 1993).

Novosad, Z. and Constain, T.G., 1990, "Experimental and modeling studies of asphaltene equilibria for a reservoir under CO_2 injection", paper SPE 20530 (Sept. 1990) 599.

Orr, F.M. Jr. et al., 1981, "Phase behavior of CO_2 an crude oil in low-temperature reservoirs", SPEJ (Aug. 1981) 480.

Pedersen, K. S., 1991, "Wax Precipitation from North Sea Crude Oils. 4. Thermodynamic Modeling", *Energy & Fuels, 1991, 5*, p. 924.

Perry and Green, 1984, *Perry's Chemical Engineering Handbook*, Sixth Edition, McGraw Hill, New York.

Rassamdana, H., 1996, "Asphalt Flocculation and Depostion: I. The Onset of Precipitation", *AIChE Journal, 42(1),* 1996, p.10.

Reid, R. C., Prausnitz, J. M. and Poling, B. E., 1987, *The Properties of Gases and Liquids*, Fourth Edition, McGraw Hill Publications, New York.

Srivastava, R.K. and Huang, S.S., 1997, "Asphaltene deposition during CO2 flooding: a laboratory assessment", paper SPE 37468 (1997) 617.

Speight, J.G., 1999, *The chemistry and technology of petroleum*, third edition, Marcel Dekker Inc., New York, NY (1999)

Srivastava, R. K. et al., 1995, "Quantification of asphaltene flocculation during miscible CO_2 flooding in the Weyburn reservoir", JCPT (Oct. 1995) 31.

Stalkup, F.I., 1978, "Carbon dioxide miscible flooding: past, present and outlook for the future", Journal of Petroleum Technology (1978) 1102.

Twu, C. H., 1984, "An internally Consistent Correlation for Predicting Critical Properties and Molecular Weight of Petroleum and Coal-Tar Liquids", Fluid Phase Equilibria, No. 6, 1984, p. 137.

Walas, 1985, *Phase Equilibria in Chemical Engineering*, Butterworth-Heinemann, Boston.

Winprop, Version 2000, *Computer Modelling Group Ltd.*, Calgary, Alberta Canada.

Won, K.W., 1985, "Continuous Thermodynamics for Solid-Liquid Equilibria: Wax Formation from Heavy Hydrocarbon Mixtures", *A.I.Ch.E. Spring National Meeting, Session 1A, March 24-28, 1985, Houston, Texas.*

Won, K.W., 1986, "Thermodynamics for Solid-Liquid-Vapor Equilibria: Wax Phase Formation from Heavy Hydrocarbon Mixtures", *Fluid Phase Equilibria, 30,* 1986, p. 265.

Won, K.W., 1989, "Thermodynamic Calculation of Cloud Point Temperatures and Wax Phase Compositions of Refined Hydrocarbon Mixtures", *Fluid Phase Equilibria, 53,* 1989, p. 377.